# Soft and Condensed Nanoparticles and Nanoformulations for Cancer Drug Delivery and Repurpose

Wen Yang, † Hanitrarimalala Veroniaina, ‡ Xiaole Qi, ‡, ¶ * Pengyu Chen†, * Feng Li§, * and Pu Chun Ke¶
†Materials Research and Education Center, Auburn University, Auburn, AL 36849, United States
‡Key Laboratory of Modern Chinese Medicines, China Pharmaceutical University, Nanjing 210009, China
¶ARC Centre of Excellence in Convergent Bio-Nano Science and Technology, Monash Institute of
Pharmaceutical Sciences, Monash University, 381 Royal Parade, Parkville, VIC 3052, Australia
§Department of Drug Discovery and Development, Harrison School of Pharmacy, Auburn University, Auburn,
AL 36849, United States

Corresponding authors: Pengyu Chen: pengyuc@auburn.edu; Feng Li: fzl0023@auburn.edu; Xiaole Qi:

xiaole.qi@monash.edu

KEYWORDS: drug delivery; nanomedicine; repurpose; tumor targeting; metal organic framework

#### **ABSTRACT**

Drug repurpose or reposition has recently been recognized as a high-performance strategy for developing therapeutic agents for cancer treatment. This approach can significantly reduce the risk of failure, shorten R&D time, and minimize cost and regulatory obstacles. On the other hand, nanotechnology-based delivery systems have been extensively investigated in cancer therapy due to their remarkable ability to overcome drug delivery challenges, enhance tumor specific targeting, and reduce toxic side effects. With increasing knowledge accumulated over the past decades, nanoparticle formulation and delivery have opened up a new avenue for repurposing drugs and demonstrated promising results in advanced cancer therapy. In this review, we summarize recent development of nano-delivery and formulation systems based on soft (i.e. DNA nanocages, nanogels and dendrimers) and condensed (i.e. noble metal nanoparticles and metal-organic frameworks) nanomaterials, as well as their theranostic applications in drug repurpose against cancer.

# **Table of Content Figure**



This review provides an account of soft and condensed nanoparticles and nanoformulations for cancer drug delivery and repurpose.

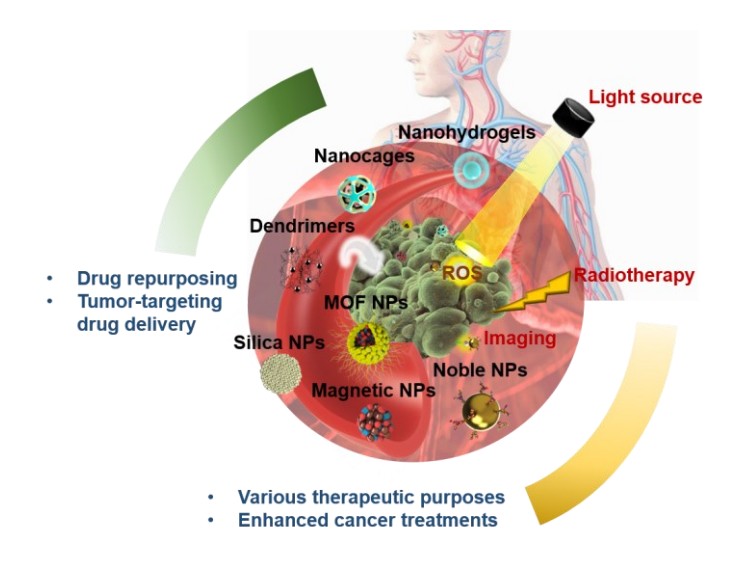
#### 1. Introduction

Cancer, characterized by abnormal growth and spread of cells in many forms, has been one of the most devastating heath concerns for decades. Cancer accounts for an estimated 9.6 million deaths in 2018 [1], making it the second leading cause of mortality, surpassed only by heart disease. Great strides have been made in recent years in medicine and technological advances. American Cancer Society reported a consecutive decline of cancer death rate since 1992 in the United States for all types of cancer and an overall decrease of 27% since its peak in 1991 [2]. A decade of research has shed new light on the underlying biology of cancer and has shifted the treatment paradigms towards a new era of cancer therapeutics.

Traditional cancer treatments such as chemotherapy, radiotherapy, and hormone therapy require high doses of drug in the tumor region with limited tumor-targeting specificity, resulting in non-selective biodistribution, damage to healthy cells or tissues, undesired cardiotoxicity and drug resistance of cancer cells [3–5]. In contrast, novel approaches such as tumor-receptor targeting, controlled drug delivery, intracellular drug targeting, gene delivery, and triggered drug release, along with continuous development in cancer drug discovery have established a valuable new set of modalities for cancer treatment [6,7]. Considering the huge cost associated with high risk of failure, significant labor and time consumption for a new drug discovery, which requires on average 13 years of research and \$1.8 billion in spending to reach a clinical application, repurposing of an approved drug for new applications has become a viable alternative in cancer drug development [8,9]. Although the repurposed or reformulated drugs still require rigorous clinical trials and regulatory approval, their risk of failure will be significantly lower than a completely new chemical entity. Furthermore, as many preclinical and clinical studies data are

available, the total development time and cost could be greatly reduced as a result of repurposing [10,11]

Recent research advances in nanomaterials and nanotechnology have spurred the development of cancer treatment, especially in tumor-targeting drug delivery, diagnosis (imaging) and nanomedicine [12–15]. Nanoparticles (NPs) exhibit a high surface-to-volume ratio, facile surface functionalization, good bioavailability, enhanced permeability and retention (EPR), and a size-dependent ability to cross the blood brain barrier (BBB), rendering them versatile nanocarriers with improved drug penetration and accumulation at tumor sites [16–18]. Conjugation of NPs with ligand-specific biomarkers such as peptides, enzymes, antibodies and DNA/RNA aptamers is a potent therapeutic approach to achieve precise targeting of cancer cells and high cancer treatment efficacy with minimal adverse effects to healthy cells [19,20]. The properties of NPs and the drug release kinetics can be well controlled by altering the size, geometry, surface function and composition of the NPs, as well as the physicochemical conditions of their surrounding environments [21,22]. In addition, NPs can serve as effective delivery vehicles to overcome the poor solubility and biocompatibility of many anticancer drugs, allowing novel nanoformulations (NFs) of anticancer drugs that have been historically unsuitable for cancer treatment [8,23].



**Schematic.** This review aims to provide the state-of-the-art in the use of soft (dendrimers, nanocages, nanohydrogels) and condensed (noble metal, silica, magnetic, and MOF) nanoparticles for cancer drug delivery and repurpose. NPs: nanoparticles. MOF: metal-organic framework.

Building on the collective promises, a wide variety of NPs have been extensively investigated and applied in pathological conditions and clinical trials [24]. Encapsulation drugs into soft NPs such as dendrimers, protein/DNA nanocages and nano-hydrogels prevents the drugs from hydrolysis or degradation, and greatly improves the solubility and bioavailability of anticancer drugs. Condensed NP-based drug delivery systems of noble metals, silicon, silica, or iron oxide with distinct physicochemical properties have shown great success in enhanced photothermal effects, X-ray and magnetic resonance imaging [15]. Metal-organic NPs (MONs) have recently drawn much attention in drug delivery due to their excellent porosity and tailorable compositions [25]. In the light of the remarkable advancements in cancer therapeutics using NPs and NFs, herein we present a review on major classes of soft/condensed NPs and NFs as novel cancer drug delivery systems and repurposing agents, in sections 2-4, and project in section 5 future opportunities for therapeutic innovations in cancer treatment (Schematic). Collectively, we wish to recapitulate the state-of-the-art nanotechnologies for novel drug delivery and better repurposed drug agents that may potentially be transformed into advanced cancer therapeutics.

# 2. Soft Nanoparticle Drug Delivery

The recent emergence of nanomedicine has promoted a great need for the development of NPs-based drug delivery. Formulating novel nanomaterials to improve their systemic circulation and tissue targeting remains a major challenge in nanomedicine. Longer circulation can result from uptake resistance through the mononuclear phagocytic system (MPS) that is comprised of the liver

and the kidney. Once reaching the systemic blood system, NPs may be recognized by the MPS as foreign substances and consequentially be eliminated. It is therefore essential to formulate NPs whose interactions with MPS organs and macrophages are well understood. Upon entering a biological fluid, the physicochemical properties of most formulated NPs are altered via the formation of a protein corona <sup>[26]</sup>, consequently resulting in altered NP aggregation and biological identity <sup>[27]</sup>. The physicochemical properties of NPs also influence their early interaction with the host's defense systems, leading to different clearance mechanisms in vivo <sup>[28]</sup>. The size and charge of the NPs play critical roles in this nonspecific binding process. For example, cationic particles are more sensible to negatively charged proteins such as glycans and phospholipids. A highly positive charge engenders interaction with the net negatively charged cell membranes to provoke cell destabilization, causing leakage of cytoplasmic proteins. A neutral surface charge of NPs can avoid macrophages uptake and consequently extend their circulation time <sup>[29]</sup>. Larger NPs are taken up more rapidly by the liver than smaller NPs. However, NPs smaller than 10 nm are eliminated quickly via glomerular filtration in the kidneys <sup>[30]</sup>.

Typically, the formulation of drug nanocarriers for cancer therapy meets two major requirements - drug encapsulation and drug release. Encapsulation of drugs in the inner cavity of a NP may avoid their pre-release until reaching the targeted tumor site and reduce the drug side effects. Stimulus-responsive drug release in a tumor microenvironment is necessary for cancer drug delivery. Soft polymeric NPs have recently become the interest of many investigations due to their potential for delivering any type of drugs. Hydrophilic, lipophilic, small and big chemotherapeutic molecules all can be encapsulated into soft NPs. Guo et al. reported that the softer the NPs, the better their drug delivery to tumors [31]. Tumor accumulation of soft NPs can result in a high drug release consequently increasing their therapeutic efficacy. Soft NPs deform

easily with modifications such as temperature and pH <sup>[32]</sup>, and are ideal templates for NP formulation since they enable interactions with drugs. Most soft NPs are biomimetic and metabolized in the human body.

#### 2.1 Drug delivery with dendrimers

Dendrimers are soft synthetic macromolecules composed of a central core with numerous branches stemming out of the core and repeating terminal groups in the outer layers. Constituted of a polar core and a polar shell, dendrimers are also termed as "unimolecular micelles" [32]. The shape and size of dendrimers can be controlled by coupling the repeating units that form their layered architecture, or "generations". Each dendrimer possesses up to 10 or more generations, displaying an increasing diameter with increasing number of generations [33]. The dendrimer core can entrap drug molecules, while the dendrimer surface groups can conjugate with functional molecules or ligands. Dendrimers are characterized by their aqueous solubility, good biocompatibility, biodegradability and general controllability, and these soft nanomaterials can enter cells via endocytosis even without carrying any drug molecules. Moreover, dendrimers are suitable for conventional drug administration through intravenous, intranasal, transdermal or ocular routes [34]. The applications of dendrimers are diverse, ranging from delivery of chemotherapeutics and imaging to photodynamic therapy, boron neutron capture and cancer gene therapy [35]. Dendrimers are synthesized with chemical methods to render different generations with a narrow molecular weight distribution, uniform size and shape, and multivalent surface groups (Figure 1). Dendrimers have been developed as theragnostic agents combining therapeutics and diagnostics in a single carrier for personalized medicine.

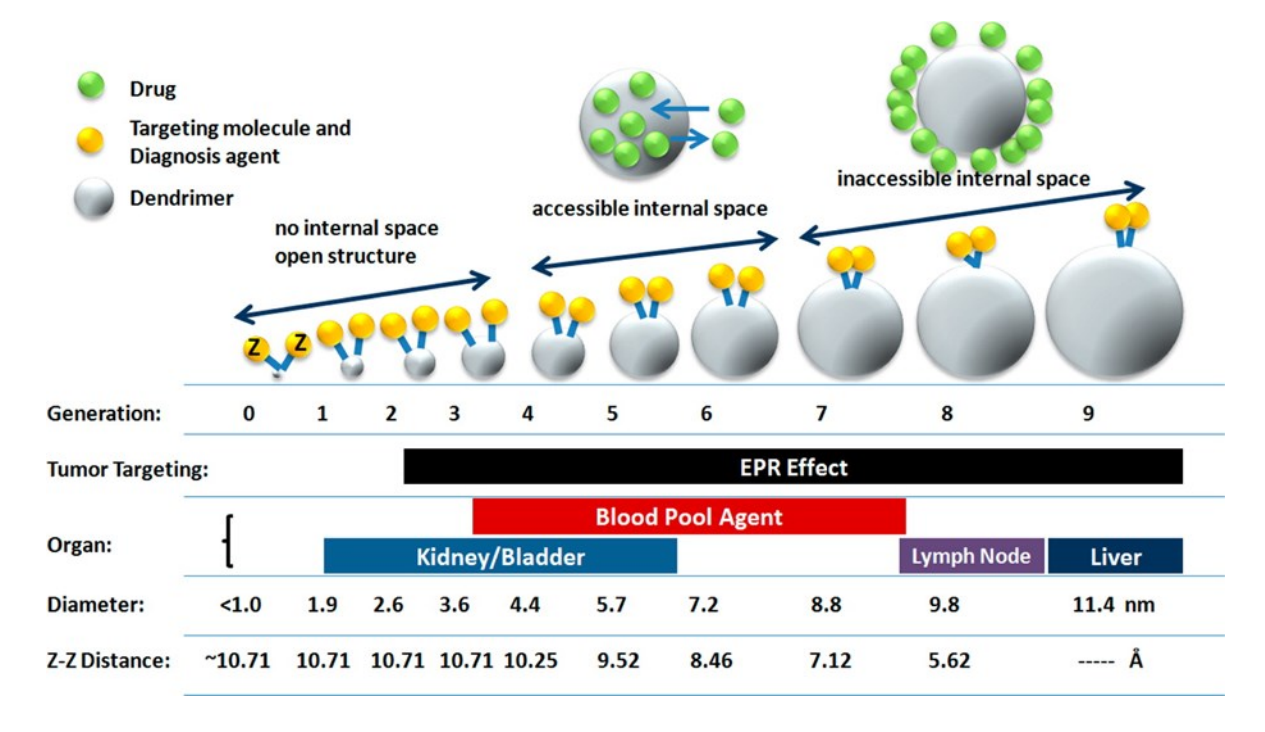


Figure 1. A dendrimer system of tunable physical properties for versatile biomedical applications. These unique features depicted here are represented by a PAMAM-DTPA (Gd) system (G0-G9) that was developed as a magnetic resonance imaging (MRI) contrast agent. Reproduced with permission from reference [36]. Copyright 2013, American Chemical Society.

Dendrimer synthesis can be performed with the divergent method where the formulation starts from the dendrimer core to the terminal groups [37], or the convergent method where the dendrimer core is integrated at the last step [38], along with other approaches such as double exponential growth [39], click chemistry [40] and "Lego" chemistry [41]. In addition, dendrimers can improve the solubility and bioavailability of their encapsulated drugs [42,43]. Drugs are stored in the inner pockets of the dendrimers through hydrogen bonds, hydrophobic or electrostatic interactions, or conjugated to the dendrimer surface groups. Chemotherapeutic drugs like doxorubicin (DOX) and tamoxifen can be encapsulated by dendrimers [44,45] via hydrogen bonding between the drugs and the -NH groups in the dendrimer interior. In addition, cationic dendrimers allow the fixation of a large amount of negatively charged drugs by electrostatic interactions with surface amino

groups. This surface ionic interaction was observed to be a major factor in the solubilization of hydrophobic drugs <sup>[46]</sup>. In the following section we summarize the more commonly used polyamidoamine (PAMAM) with an ethylenediamine core, poly(propylene imine) (PPI) with a 1,4-diaminobutane core and Poly-L-lysine (PLL) with a Boc-l-Lys(Boc)-OH benzhydrylamide core <sup>[47]</sup>.

#### 2.1.1 PAMAM dendrimers

PAMAM dendrimers, first reported by Tomalia in 1985, are mostly employed for drug delivery [37]. This class of dendrimers possesses strong hydrophilicity, biocompatibility and non-immunogenicity. PAMAM are synthesized by a divergent method in which methyl acrylate and ethylenediamine are used as the branching units, and their terminated groups contain amines (for full generations) or carboxyls (for half generations) [48]. Generally, high-generation (G4 or higher) PAMAM dendrimers provide a large space to encapsulate drugs via physical or chemical interactions [49]. Numerous studies have shown that the binding, release and biocompatibility of PAMAM can be attributed to their surface amines [50,51], and modifications of the terminal functionalities of PAMAM may therefore improve their encapsulation efficiency, pharmacokinetics, solubility, toxicity, stability as well as drug release efficiency [52]. Multiple anticancer drugs have been loaded within PAMAM, including cisplatin [53], DOX [54], adryamicin, methotrexate [55] and 5-fluorouracil [56].

#### 2.1.2 PPI dendrimers

Poly(propylene) imine (PPI) dendrimers were first formulated by Meijer et al. in 1993 [57] via a divergent method. Compared with PAMAM, PPI are more hydrophobic since they possess alkyl chains in their branching units from propylene imine monomers [58] and are smaller due to the

shorter branching units. Shao et al. compared the drug loading ability, release behavior and cytotoxicity of G3 PAMAM and G4 PPI dendrimers [58] using phenylbutazone as a model drug. G3 PAMAM dendrimers were advantageous in solubility and drug release and were one order of magnitude less toxic than G4 PPI dendrimers to MCF-7 and A549 cells (Figure 2A). Maculewicz et al. modified the surface of PPI dendrimers with maltose residues (PPI-m) and loaded the dendrimers with cytarabine [59], a drug of nucleoside analogues (NAs) commonly used to treat acute myeloid leukemia, acute lymphocytic leukemia and lymphomas. The PPI-m dendrimers enhanced acute cytotoxicity against a myeloid leukemia cell line 1301 in comparison with free cytarabine. Thus, PPI-m dendrimers improved the stability of NAs and efficiently delivered the active drug directly to cancer cells.

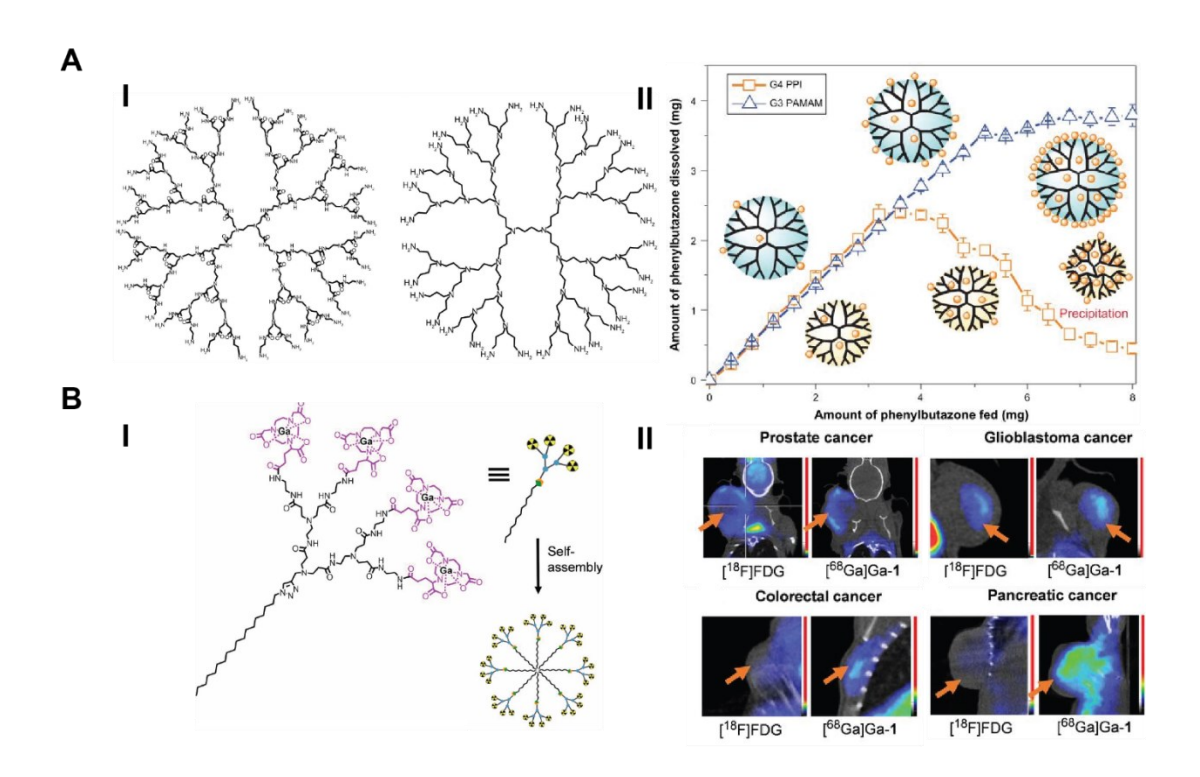


**Figure 2. Drug delivery with dendrimers.** A. Comparation between PAMAM and PPI dendrimers. I) Molecular structures of PAMAM (left) and PPI (right) dendrimers. II) Drug-loading capacities of G3 PAMAM and G4 PPI dendrimers determined by a gradient-feed method <sup>[58]</sup>. Copyright 2011, Dove Medical Press Ltd. B. A dendrimer nanosystem based on a self-assembling amphiphilic dendrimer bearing

radionuclide terminals for PET imaging of tumors. I) A self-assembling amphiphilic dendrimer bearing radionuclide terminals for PET imaging of tumors. II) A radiolabeled dendrimer for PET imaging of various tumors, where [<sup>18</sup>F] FDG is a clinical gold standard for PET imaging in oncology and orange arrows indicated tumor positions [<sup>60]</sup>. Copyright 2018, National Academy of Sciences.

#### 2.1.3 PLL and CCD dendrimers

Poly(lysine) (PLL) dendrimers are mostly asymmetrical with amino acid lysine in their core and branching units and amines as terminal residues. PLL dendrimers as nanocarriers possess an innate antiangiogenic efficacy without loading any therapeutic drug <sup>[61]</sup>. Cationic PLL dendrimers associated with DOX led to a deeper penetration in 3D tumor spheroid models tested with DU145 prostate cancer cells <sup>[62]</sup>, utilizing the small size (<10 nm) and surface positive charge of the dendrimers <sup>[63,64]</sup>. Compared with free DOX, the PLL dendrimers-DOX complexes elicited significant tumor suppression after a single intravenous injection.

Despite their great potential for drug delivery, the usage of dendrimers is limited by their hemolytic and toxic effects due to the type of the core and especially the strong cationic charge of the surface end groups <sup>[65]</sup>. The surface of dendrimers can be easily modified either to improve tumor targeting or attach an imaging agent. Conjugating polyethylene glycol (PEG) with dendrimers has been a common method to enhance circulation and tumor accumulation via the EPR effect <sup>[56,66]</sup>. Besides, carbosilane copper dendrimers (CCDs) are newly formulated NPs having chloride and nitrate ligands on the surfaces for cancer therapy <sup>[67]</sup>. Concerning cytotoxicity, dendrimers with chloride ligands were more efficient than those with nitrate. CCDs have the ability to distinguish tumor cells from normal cells and show significant cytotoxicity. Philippe et al. <sup>[60]</sup> recently formulated a self-assembled nanosystem for positron emission tomography (PET) imaging, based on an amphiphilic dendrimer which had multiple PET reporting units at its terminals. Combining dendrimeric multivalence and EPR-mediated passive tumor targeting, this

nanosystem demonstrated superior imaging sensitivity and specificity (**Figure 2B**). Starpharma has developed PEGylated PLL dendrimers surface-attached with docetaxel, namely, DEP® docetaxel [31b]. This formulation is currently in Phase II clinical trials for lung and prostate cancers. The phase 1 results demonstrated a remarkable capacity of the dendrimers in delivering drugs by reducing the latter's life-threatening and dose-limiting toxicity. The NF displayed a superior anti-cancer activity than free docetaxel.

#### 2.1.4 Dendrimer-like polymers

Nano-star polymers consist of several linear polymer chains connected to a central core. Their physicochemical properties can be tailored by branched polymer arms of specific functionality [68]. Besides, the stimulus-responsive micellization properties and high drug-loading efficiency enable nano-star polymers controllable nanocarriers for drug delivery. Depending on configuration and composition differences, star polymers can be divided into two categories: homo-arm star polymers possessing symmetric arms with identical chemical composition and structure, and miktoarm polymers consisting of at least two different arm species with different compositions or molecular weights [69]. Among these, amphiphilic star polymers with a hydrophobic core and hydrophilic chains have been investigated extensively as nanocarriers for drug delivery. Such amphiphilic structures can self assemble in aqueous solutions to form nano-ordered micelles and encapsulate hydrophobic drugs or poorly soluble molecules into the core. The core segments of the star polymers are usually biodegradable to avoid drug accumulations for a long term. Chong et al. investigated a series of PLGA-AAA-(mPEG)<sub>2</sub> miktoarm star polymers possessing monomethoxy poly(ethylene glycol) (mPEG) of 2 kDa with different molecular weights of poly(lactide-co-glycolide) (PLGA) arms. Miktoarm star polymers PLGA-AAA(mPEG)2 with low molecular weight of PLGA(4.6 kDa) self-assembled into stable nanomicelles, while PLGA17.0AAA(mPEG)<sub>2</sub> and PLGA43.4-AAA(mPEG)<sub>2</sub> formed stable NPs. All of them exhibited a dual-stage drug release and a great potential for hydrophobic drug delivery <sup>[70]</sup>. Alonso-Cristobal et al. synthesized an amphiphilic star-shaped block copolymer with branched poly(ε-caprolactone) as the hydrophobic core and branched poly(ethyleneglycol) as the hydrophilic corona <sup>[71]</sup>. Liu et al. designed a cyclodextrin derivative (CD-PLLD) consisting of a cyclodextrin core and poly(l-lysine) dendron arms to achieve simultaneous delivery of hydrophobic anticancer drugs DOX and MMP-9 siRNA plasmid gene in vivo <sup>[72]</sup>.

#### 2.2 Drug delivery with ferritin-based protein nanocages

Ferritin, a ubiquitously expressed protein observed in bacteria, archaea and eukaryotes for the purpose of iron storage, is an archetypal example of protein-based NPs and one of the most investigated proteins. The inner cavity of ferritin can store up to 4,500 Fe (III) atoms [73]. In eukaryotes, a spherical ferritin nanocage consists of 24 self-assembled subunits of heavy and light peptide chains. Two types of ferritin, H-ferritin and L-ferritin are formed by heavy (H; 21 kDa) and light (L; 19 kDa) chains, respectively [74]. To enter cells, H-ferritin binds with transferrin receptor 1 (TfR1) [75] or the T-cell immunoglobulin domain and mucin domain-1 (TIM-1) [76], while L-ferritin binds with scavenger receptor class A member 5 (SCARA5) [75,77]. Naturally, the inner cavity of ferritin is loaded with iron. When expressed in iron-free conditions, a hollow cage of apoferritin is rendered. The iron core can be removed with suitable reducing and chelating agents such as sodium dithionite and EDTA, or BIPY [78]. Apoferritin has cavities in the center to accommodate molecular cargos and serve as a biological template for NPs [79]. Indeed, NPs constructed by the heavy chains of ferritin (HFn) have been in development for drug delivery, exploiting overexpression of TfR1 in most tumor cells for endocytosis. Moreover, ferritins are

characterized by their biodegradability, water solubility, versatile functionalization and drug loading capacity [80,81], and have been developed for oncology drug delivery thanks to their stability and excellent particle uniformity (outer diameter of 12 nm, inner cavity of 8 nm) [82]. This size is perfect to avoid elimination by the kidney (>10 nm) and can take advantage of the EPR to increase tumor-targeted drug delivery.

Various studies have used ferritin as a drug delivery platform by encapsulating therapeutics drugs and integrating targeting molecules on its surface. According to electrostatic gradient calculations, the outer surface of ferritin is positive, and the inner surface is negative [83]. Ferritin drug loading can be achieved via pH-induced disassembly/reassembly [84], diffusion through the surface pores, and direct conjugation of drugs to the ferritin surface. The ferritin nanocage can be disintegrated at pH 2 and the subunits can be reconstituted at pH 7.4 [85], thereby avoiding prerelease during systematic circulation. The uniform size of the nanocage ensures high reproducibility of cargo encapsulation. In addition, the presence of eight hydrophilic 3-fold pores and six hydrophobic 4-fold pores in the protein shell facilitates the entry and exit of iron and other cations [86]. The surface of an apoferritin cage has abundant amines, which can be modified genetically or chemically to conjugate targeted ligands to entail multifunctionality and versatility to ferritin. Compared with other protein nanocarriers, ferritin can withstand temperatures up to 80-100 °C and pH 3-10. Upon binding TfR1 on the cell surface, the H-ferritin-TfR1 complex is internalized following receptor-mediated endocytosis. The acidification of endosomes can trigger a gradual release of the ferritin cargo. Furthermore, payload release can be controlled via a pH trigger [87], temperature [88], reactive oxygen species (ROS) [89] (**Figure 3A**) or ultrasound [90].

Ferritin has been studied extensively as a carrier for drug delivery since 2005 [91]. For cancer therapy, ferritin nanocages have been loaded with small molecules such as DOX [92],

cisplatin [93] and daunorubicin. Encapsulation of cancer drugs in apoferritin enhances their tumor accumulation and cytotoxicity due to targeted release. Ferritin-based lung inhalation delivery system has been designed to improve lung mucus penetration and enhance targeting of lung tumor tissue [94]. Ferritin nanocages with PEGylation penetrated airway mucus and the tumor tissue barrier. The newly formulated NPs showed a selective uptake by cancer cells, and drug release was activated upon cell uptake. Ferritin-based drug delivery crossed the blood brain barrier (BBB) to target brain tumor [95] due to the high expression of TfR1 in both brain endothelial and glioma cells. Surface shell modification is a common strategy to improve the performance of ferritin NPs. For example, DOX was encapsulated within an apoferritin nanocage equipped with a gold (Au) nanoshell to achieve multi-stimuli responsive drug release [96]. The nanocage displayed a photothermal effect due to surface plasmon resonance (SPR) associated with the Au nanoshell, increasing its sensitivity for changes in pH and temperature to improve tumor drug release. In a separate study, Prussian Blue-modified ferritin NPs (PB-Ft NPs) [97] fused the photothermal conversion property of PB with the tumor targeting capacity of ferritin. The PB-Ft NPs inhibited the growth of murine breast cancer cell line (4T1) and improved the therapeutic activity of gemcitabine (GEM) by increasing ROS production, thereby implicating the NPs as a tumor chemotherapeutic sensitizer and a photothermal therapy reagent. Furthermore, to avoid the short plasma half-life (~2 h) associated with most protein-based NPs [81], an albumin binding domain (ABD) has been fused to the N-terminus of HFn for half-life extension [84]. The anti-tumor drug DOX was encapsulated in the ABD-HFn complex, and pharmacokinetics characterizations indicated a significantly prolonged plasma half-life of ~17.2 h.

Apoferritin NPs can also target cell lines expressing epidermal growth factor receptor (EGFR) after incorporating targeting ligands on their surfaces. Oxaliplatin-loaded apoferritin has

been conjugated with panitumumab (AFPO) <sup>[98]</sup>. The anti-cancer activity of AFPO has been confirmed after great tumor accumulation into cells overexpressing EGFR and release of oxaliplatin. Moreover, apoferritin surface functionalized with folic acid (FA) enhanced its cellular uptake via FA-receptor-mediated endocytosis <sup>[85]</sup>.

Table 1. Recent ferritin-based drug delivery for cancer treatment.

Year	Ferritin nanoparticles	Cancer type tested	Findings	References
2019	Prussian blue and gemeitabine-loaded ferritin	Breast cancer 4T1 cells line	Chemo-photothermal combination therapy	[97]
2019	DOX-loaded apoferritin surface-modified with gold nanoshell	Hepa1-6cells line	Multi-stimuli responsive drug release (pH, temperature)	[96]
2018	Benzothiazole	Breast, renal and ovarian cells line	High drug loading of 380 molecules per apoferritin cage	[99]
2019	Ellipticine-loaded apoferritin	UKF-NB-4 neuroblastoma cells	Therapeutic efficacy for neuroblastoma treatment	[100]
2018	Oxaliplatin-loaded apoferritin conjugated with panitumumab	Colorectal cancer	Targeting tumor cells overexpressed with epidermal growth factor receptor (EGFR)	[98]
2018	Epirubicin-loaded apoferritin surface- modified with folic acid	MCF-7 breast cancer cells	Improving cellular uptake of apoferritin	[85]

Iron oxide NPs formulated within a ferritin cage have been exploited in targeted drug delivery and bioimaging of cancer cells [101]. Lin et al. developed a multifunctional imaging system with Cy5.5 conjugated to a matrix metalloproteinase (MMP) cleavable peptide and a BHQ-3 quencher [102]. Kitagawa et al. demonstrated dual near-infrared fluorescence (NIRF) and MRI imaging of tumor [103]. An arginine-glycine-aspartic acid (RGD) targeting moiety has been incorporated to ferritin for imaging vascular inflammation and angiogenesis. Compared with conventional nanocarriers, ferritin nanocages are safe and biocompatible materials for theranostics. Lately, the theranostic efficiency of Gd- and curcumin-encapsulated apoferritin (Apo-CUR-Gd)

was evaluated on cancer stem cells <sup>[77]</sup>. This theranostic complex improved the bioavailability of curcumin and tumor targeting, impaired the cell viability and self-renewal of tumor spheres, and consequently led to diminution of tumor volume in mice.

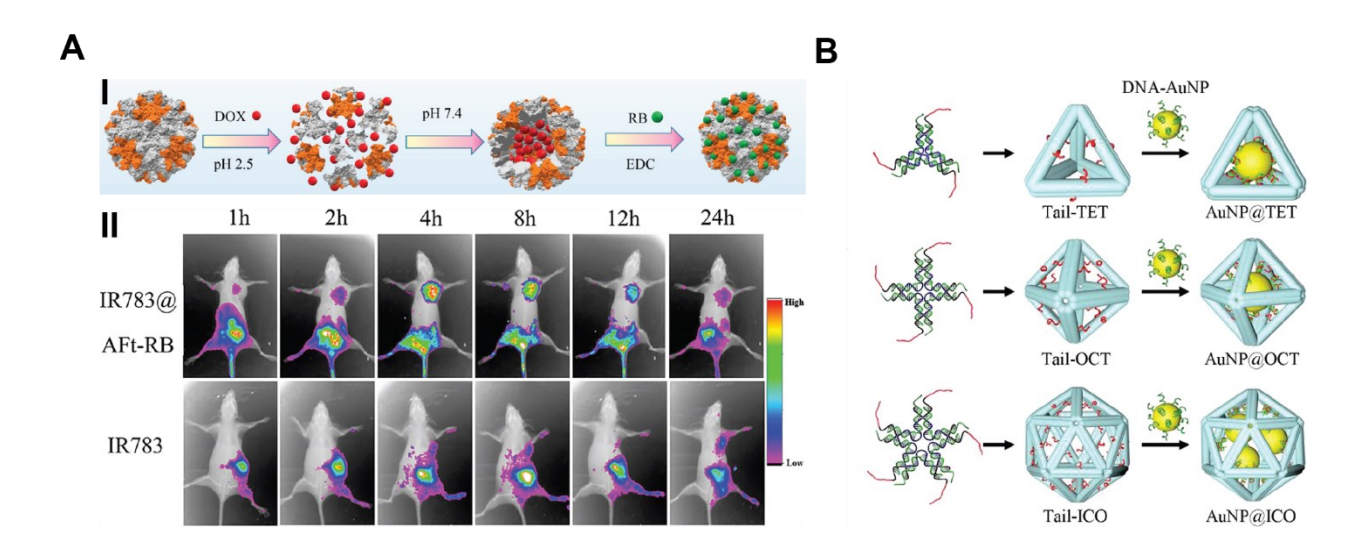


Figure 3. Apoferritin and DNA nanocages in drug delivery. A. Apoferritin nanocage for ROS/pH-controlled drug delivery to breast cancer. I) Schematic for DOX@AFt-RB synthesis, where Aft denotes apoferritin and RB represents photosensitizer rose bengal. The drugs release occurs at low pH and with laser radiation. II) In vivo fluorescence imaging showed no specific localization for the free near-infrared dye IR783 group. However, DOX@AFt-RB showed a good tumor targeting effect and exhibited stronger fluorescence in the tumor regions [89]. Copyright 2018, American Chemical Society. B. DNA polyhedra encapsulated AuNPs to form core-shell structures (AuNP@cages). The number of AuNPs encased by a DNA cage depended on the inner volume of the DNA cage [104]. Copyright 2014, American Chemical Society.

#### 2.3 Drug delivery with DNA nanocages

DNA nanocages entail several functions such as drug delivery, imaging and biosensing. DNA-based drug delivery can target tumor site, enter cancer cells, oppose enzymatic degradation and defeat multidrug resistance. There are two major types of DNA nanocages: pure DNA nanostructures and hybrid DNA nanostructures of 10 to 100 nm in size. Specifically, pure DNA

nanostructures include DNA polyhedrons, DNA nanoribbons, DNA module assemblies, DNA nanoflowers and DNA origamis, while hybrid DNA nanostructures encompass DNA-inorganic NP hybrids, DNA-lipid hybrids and DNA-polymer hybrids.

DNA-based drug delivery enhances tumor accumulation because of the EPR effect. In addition, self-assembly, biocompatibility and biodegradability are notable advantages of DNA nanocages over other nanocarriers. DNA nanocages can be assembled via: (1) a one-pot approach in which the cages are manufactured all at once, (2) modular assembly in which multiple components are first synthesized then integrated inside the target DNA nanocages, (3) hierarchical self-assembly in which a specific DNA tile sticks to higher-order DNA structures and (4) DNA origami in which a long single-stranded scaffold is folded into a desired cage structure by the addition of short complementary staple strands [105].

DNA nanocarriers are smart delivery devices for molecular cargos. DNA nanocages can also serve as a host to encapsulate existing NPs. The guest-host interaction between DNA nanocages and inorganic NPs is a viable strategy to combine properties intrinsic to DNA and characteristics of inorganic NPs. AuNPs were successfully incorporated within polyhedral DNA nanocages and formed a DNA cage core-like structure [104] (**Figure 3B**). The DNA nanocages as a host ensured a controllable release of AuNPs.

#### 2.4 Drug delivery with nano-hydrogels

Nanohydrogels have recently been explored for cancer drug delivery. Hydrogels are molecules formed of hydrophilic polymer chains that are flexible, biocompatible and biodegradable [106]. Hydrogels can be grouped according to the types of polymers, methods of synthesis, stimuli-responsiveness, or the nature of cross-linking for establishing the three-dimensional network of the polymer chains. Nanohydrogel-based NPs may be prepared from natural materials such as

proteins, polysaccharides and DNA to ensure biocompatibility, or from the polymerization of synthetic monomers to entail good functionality. Mixing natural and synthetic polymers can render biohybrid hydrogels [107,108]. Hydrogels can also be classified into chemical and physical hydrogels, where chemical hydrogels involve covalent cross-linking, while physical hydrogels are built upon the self-assembly of polymer chains via hydrogen bonding or hydrophobic interaction. Physical hydrogels can be synthesized with a reversible process using pH, solvent or temperature. Owing to their rich content in water, hydrogels acquire their high biocompatibility and biodegradability [109]. Hydrogels are sensitive to environmental changes such as pH, temperature, ionic strength and light, which can result in their compression or swelling leading to drug release. Nanohydrogels combine the advantages of hydrogels and NPs. Their swelling ability, for example, depends on the number of ionic groups. The elasticity of nanohydrogels is necessary to resume their original shape after the discharge of force applied during synthesis. Nanohydrogels are mostly formed with natural polymers such as chitosan, cellulose, alginate, pectin, dextran and hyaluronic acid (HA). However, synthetic nanohydrogels can be formulated with poly(vinyl alcohol) (PVA), poly(ethylene oxide) (PEO), poly(ethyleneimine) (PEI), and poly(vinyl pyrrolidone) (PVP) approved by FDA as nonantigenic in nature [110]. Nanohydrogels gels can be formulated by various approaches, most notably by emulsion polymerization, where free radical polymerization has been used as the process methodology.

Drug loading in nanohydrogels is based on covalent and noncovalent interactions, or physical entrapment. The nanoscale of nanohydrogels allows them to avoid elimination by the kidney and the liver, thereby increasing their blood circulation. Longer circulation further enables the use of drugs at a lower dose, which is desirable for drug delivery [111,112]. Interestingly, nanohydrogels are able to incorporate a large amount of either hydrophilic or hydrophobic drugs

within the spaces in the polymeric chains. They are known not only for their rapid drug delivery, especially hydrophobic drugs, but also for their ability to reach deep tissues <sup>[113]</sup>. Recently, Becher et al. developed a new hybrid nanohydrogel drug delivery platform based on laponite nanodiscs (**Figure 4**) <sup>[114]</sup>. This newly formulated nanohydrogel encapsulated several cancer drugs with an efficient drug cocktail delivery system. The facile formulation rendered a significant anti-tumor activity and a lower cytotoxicity.

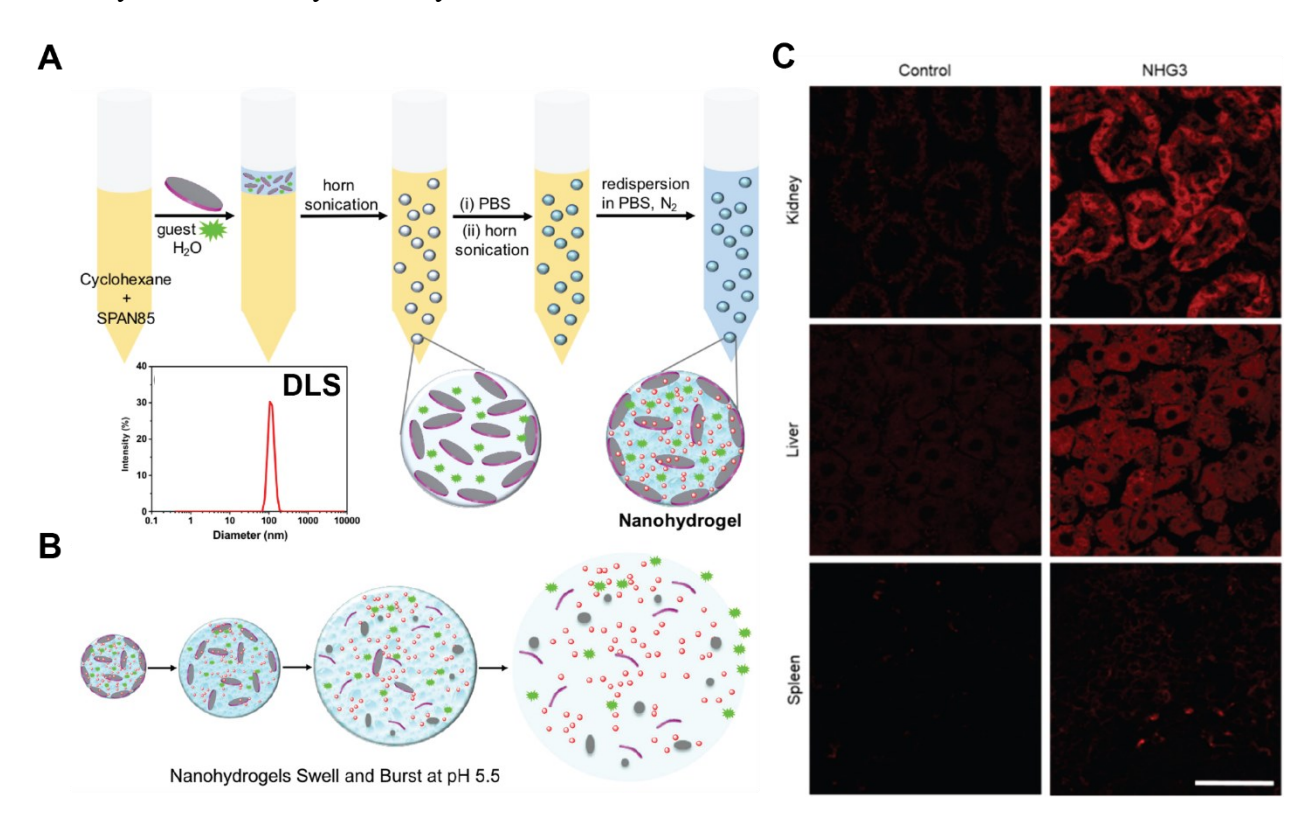


Figure 4. Nanohydrogel-based drug delivery platform against MCF-7 cells. A. Schematic for nanohydrogel synthesis using a nanoemulsion template procedure. The dynamic light scattering (DLS) data showed the size distribution of nanohydrogels in the range of 80-180 nm. B. The swell and burst processes of nanohydrogels occurring at pH 5.5. C. Confocal fluorescence microscopy (CFM) images showed that nanohydrogels were mainly distributed in the kidney and liver but no change of biochemical markers in these organs was observed. Scale bar =  $50 \mu m$  [114]. Copyright 2018, American Chemical Society.

Drug repurposing is a strategy to provide a novel therapeutic indication from an existing drug which failed its original indication. There are many approaches to repurpose a conventional

drug such as pharmacological analysis, retrospective clinical analysis, genetic association, pathway mapping, signature matching and molecular docking<sup>[11]</sup>. As many studies have indicated, changing the route of drug administration from the original mode is a method for drug repurposing. This strategy can improve the bioavailability and avoid the original side effects by encapsulating the repurposed drug within NPs <sup>[115–120]</sup>. Notably, this system can deliver the repurposed drugs alone or combined with other drugs to enhance the therapeutic index with a single nanocarrier that is important in drug repurposing. In that regard, soft NPs may guide advancement in drug repurposing for cancer diagnostics and treatment.

### 3. Condensed Nanoparticles for Drug Delivery and Cancer Therapy

Condensed NPs such as noble metal, silicon, silica and iron oxide have drawn much attention in drug delivery and cancer therapy. Their improved solubility, biocompatibility, customized surface and multi-functionality enable them to interact with complex cellular functions for improved therapeutic efficiency, leading to wide biomedical applications [121–123]. Here, we review typical condensed NPs and their applications in drug repurposing, delivery and cancer therapy improvement.

## 3.1 Noble metal nanoparticles

Noble metal NPs are widely used in biomedical applications owing to their unique physical and chemical properties, such as ease of synthesis, facile surface modification and good biocompatibility. Noble metal NPs can be easily functionalized with various biomolecules or biocompatible polymers, such as peptides [124], enzymes [125], antibodies [126] and DNA/RNA aptamers [127], to form noble metal NP-biomolecular conjugates. The biomolecules introduced to

noble metal NPs surfaces can specifically target different types of cells, thereby enabling the NPs to act as therapeutic carriers or chemotherapeutic agents. In addition, noble metal NPs possess a unique optical property of localized surface plasmon resonance (LSPR), which arises when incident light with specific wavelength couples with the oscillation frequency of the electrons on noble-metal NP surface to induce a strong absorption band and enhance photo-to-heat conversion [128,129]. The optical properties of noble metal NPs can be easily tuned via designed geometry, size and composition, to restrict LSPR absorption band into the near infrared (NIR) range where native tissues and water molecules have minimal absorption and scattering, leading to maximum tissue penetration of light and strong photothermal effects to improve the cancer therapy [130]. Gold, silver and platinum are most investigated noble metal materials in biomedical research. In particular, AuNPs have been employed for cancer therapy and diagnostics, AgNPs for antibacterial, and Pt-NPs for scavenging ROS to catalyze biological reactions. In the following sections, we present noble metal NP-based drug repurposing and delivery systems for cancer treatment [131].

#### 3.1.1 Noble metal nanoparticles for anticancer/non-anticancer drug repurposing

Platinum-containing drugs, such as cisplatin, carboplatin and oxaliplatin, are most widely exploited chemotherapeutic agents for cancer treatment due to their electro-catalytic properties. However, undesired side effects including nephrotoxicity, neurotoxicity, ototoxicity, bone marrow suppression and drug resistance are major restrictions in their use [132]. It is therefore of urgency to develop a new generation of anticancer drugs with good selective toxicity on tumor cells and to mitigate drug resistance. Repurposing existed anticancer/non-anticancer drugs and enhancing drug efficiency by incorporating NPs have proven to be one of the powerful tools to overcome clinical drug resistance.

DOX is a commonly used chemotherapeutic drug for the treatment of breast cancer, leukemia and lymphoma [133]. DOX intercalates with DNA and suppresses macromolecular biosynthesis in cancer cells. However, undesirable traits restrict the clinical use of DOX in the treatment of brain cancer. First, the BBB is impermeable to almost all the anti-cancer drugs [134]. Even though DOX has demonstrated potent cytotoxicity to glioma cells, its impenetrability to the BBB and short plasma half-life yield poor performance in brain tumor treatment. Etame et al. used an in-vitro model to investigate the size-dependent EPR effect of AuNPs (4-24 nm) with the surface modification of PEG of various chain lengths (1000-10,000 Da in M.W.), where the smallest AuNPs modified with low M.W. PEG displayed an optimum permeation of the brain microvasculature<sup>[135]</sup>. Dhar et al. demonstrated the concentration-related cytotoxicity of DOXloaded-gellan gum-reduced AuNPs in human glioma cell lines. Compared to free DOX that relies on passive diffusion, the improved drug uptake by endocytosis of DOX-load AuNPs rendered increased cytotoxicity and inhibition of cancer cell viability in vitro [136]. Cheng et al. demonstrated transactivator of transcription (TAT) peptide-modified AuNPs (5 nm) as an efficient platform for anti-cancer drug delivery across the BBB. The accumulation of TAT-modified PEGylated AuNPs (TAT-AuNPs) in brain tumor was dramatically increased in vivo compared to PEGylated AuNPs due to TAT-mediated transcytosis. In addition, TAT-AuNP-DOX did no harm to healthy organs, and no morphological changes of the tissues were observed in 6 weeks while the AuNPs were cleared through renal excretion. The DOX-conjugated TAT-AuNPs delivery system showed enhanced cytotoxicity and cellular uptake in several glioma cell lines than free DOX in vitro and in vivo [134] (Figure 5A).

The failure of DOX in colorectal cancer (CRS) treatment is mainly due to the development of drug resistance and cardiotoxicity. Although DOX is an efficient chemotherapy drug for CRS

at advanced stages, high dosage of the drug used in the therapy can result in multidrug resistance of CRS. Accordingly, DOX loading onto AuNPs provides a possible way to improve the therapy in CRS. The high surface-area-ratio and facile molecular modification of AuNPs enable a tunable dose adherence of the loaded drug and controllable drug release. Lee et al. found that immobilized oligonucleotides (ONT) on the surface of AuNPs (13 nm) provided numerous binding sites and greatly increased DOX loading through intercalation. The DOX-loaded AuNPs (DOA) elicited significant cytotoxicity at relatively low concentrations and slow drug release (only 28% of DOX was released after 100 h). The enhanced local drug release can greatly prevent high dose-induced drug resistance<sup>[137]</sup>. Benyettou et al. coated AgNPs with DOX and alendronate (Ald) to investigate their anticancer activity in HeLa cell lines. Ald is a potent bisphosphonate that can not only synergistically act with DOX to enhance the antitumor effect, but also provide an attachment for DOX on AgNPs through the ammonium group. Acidic environments can induce hydrolysis of the imine-linkage between DOX and Ald, leading to drug release. This synergistic drug delivery platform entailed reduced drug dosing, minimized toxicity to normal tissues, and prevented drug resistance [138].

DOX-induced heart failures are another important constraint for the utility of DOX in cancer therapy [139]. Compared with other organs, the heart is more vulnerable to increased oxidative stress. Indeed, DOX-induced cardiotoxicity is one of the most serious side effects related to ROS-induced oxidative stress. PtNPs can reduce intracellular ROS and decrease the risk of chemotherapy drug-induced oxidative stress in normal tissues and alleviate cardiotoxicity. Yang et al. constructed cRGD-coated porous Au@Pt bimetallic for DOX delivery. The ROS-scavenging activity of Au@Pt has been demonstrated in vivo, where porous Au@Pt NPs alleviated DOX-induced oxidative stress and reduced the risk of cardiomyopathy during chemotherapy [140]. Yusof

et al. examined the antioxidant effect of PtNPs in lung cells and found that PtNPs reduced ROS generation and decreased cellular oxygen species, which suggested that PtNPs could sustain oxidation and stimulate lung liquid clearance in the treatment of lung diseases [141].

Curcumin (1,7-bis(4-hydroxy-3-methoxyphenyl)-1,6-heptadiene-3,5-dione), a polyphenol derived from turmeric of the Curcuma longa, has long been used as both a food and a medicine over 4,500 years in Asia. Ancient Indians used curcumin to treat common infections induced by wounds, bites, burns and skin diseases [142,143]. Numerous in vitro and in vivo studies have demonstrated various pharmacological activities of curcumin, such as anti-inflammatory, antioxidant, antibacterial, antifungal and antiviral properties. Curcumin has attracted increased attention since 1990s, when Aggarwal et al. reported the potential anticancer effect of the polyphenol [144]. Although curcumin exhibits significant biological properties, its therapeutic applications are greatly restricted due to its poor bioavailability, low solubility, rapid systemic elimination, and limited targeting specificity. Loading curcumin on metal NPs, especially AuNPs, has been demonstrated effective to improve the biocompatibility of curcumin due to the low toxicity and high bioavailability of AuNPs [145]. Gangwar et al. reported that PVP could be used to facilitate the conjugation of curcumin with AuNPs and improve the solubility of curcumin in water [146]. Sindhu et al. prepared curcumin-conjugated AuNPs (cAuNPs) at room temperature and solubilized curcumin without using any external agent. The cAuNPs displayed good stability and non-toxicity to human blood cells at micromolar concentrations [147]. Garg et al. used a curcumin extract to reduce silver ions by encapsulating curcumin in the AgNPs. Curcumin induced cytotoxicity to tumor cells in a dose-dependent manner and elicited a greater antitumor effect than plain curcumin [148]. AgNPs improved the bioavailability and enhanced the anticancer activity of curcumin towards cancer cell lines. Compared to widely used physical- and chemical synthesis

protocols which require considerable time and cost with relative low yields and usually involve chemical reducing agents such as citrate, borohydride and non-biodegradable polymers, using biological synthesis methods provide more effective and environment-friendly ways to rapidly synthesize biocompatible noble metal NPs.

Temozolomide (TMZ) is a chemotherapeutic agent used in the clinical treatment of various cancers, especially melanoma and glioblastoma. Increased interest in TMZ has been generated due to the chemoresistance of cancer cells to conventional cisplatin-related drugs. Hamzawy et al. developed AuNPs and liposome-embedded AuNPs (LGNPs) as drug carriers for TMZ to treat urethane-induced lung cancer in a BALB/c mouse model through intratracheal inhalation and proved an enhanced drug efficacy associated with reduced systemic toxicities of TMZ-loaded AuNPs (TGNPs) and liposome-embedded TGNPs (LTGNPs). AuNPs increased cell penetration, thereby inducing apoptosis and necrosis in lung cancer cells due to ROS generation and cellular glutathione regulation [149].

#### 3.1.2 Anti-cancer properties of noble metal nanoparticles

Apart from corporation with anti-cancer drugs, some noble metal NPs have their own antitumor properties. AgNPs have been investigated against human hepatoma <sup>[150]</sup>, lung cancer <sup>[151]</sup>, breast cancer <sup>[152]</sup> and cervical carcinoma cells and proven to possess tumor inhibition and antitumor effects <sup>[153]</sup>. Franco-Molina et al. observed a dose-dependent cytotoxic effect of colloidal silver on MCF-7 breast cancer cells through induction of apoptosis, but not on normal PBMC cells <sup>[154]</sup>. Guo et al. found that PVP-coated AgNPs possessed an anti-leukemia activity via ROS generation and silver ion release <sup>[155]</sup>. Asharani et al. reported that the reaction between  $H_2O_2$  and AgNPs was causative to induce silver ion release in vivo through chemical reaction:  $2Ag + H_2O_2 + 2H^+ \rightarrow$ 

 $2Ag^{+} + 2H_{2}O$ , where standard reduction potential  $E_{\theta} = 0.17$  V. The released  $Ag^{+}$  ions interacted with thiol-containing proteins and molecules in the cytoplasm, cell membranes and inner membranes of mitochondria, resulting in lipid peroxides and increased cell membrane permeation. It has been found that cell membrane damage can cause leakage of cytoplasmic contents and eventual necrosis, lysosomal membrane damage can lead to cathepsin release and induce apoptosis, while mitochondria damage can impair electron transfer, inhibit adenosine triphosphate (ATP) synthesis, increase ROS generation, and DNA damage and cell death (Figure 5B) [153,156–158]. PtNPs were non-toxic at therapeutically relevant concentrations, whereas laser irradiation enabled PtNPs to efficiently kill human cancer cells. The surfaces of irradiated individual PtNPs of 50-70 nm in size rose up to 900 K due to their good thermal stability, whereas gold nanoshells (AuNSs) underwent a structural change when temperature reached around 400 K<sup>[159]</sup>. Small-sized Pt nanoclusters (~2.5 nm) could efficiently overcome the chemoresistance and heterogeneous stemness of HCC cells by modulating genes related to the cell cycles and DNA damage pathways. [160]. Peptide-coated PtNPs induced significantly more toxicity than cisplatin against liver cancer cells, but had little effect on other cancer or non-cancerous cells even with increased particle internalization. The higher oxidative state in liver cancer cells provided a high ROS concentration, which oxidized inert Pt<sup>0</sup> to Pt<sup>II</sup> to render cytotoxicity and DNA damage, determined by combined high cellular uptake and an oxidative environment [161].

#### 3.1.3 Noble metal nanoparticles for cancer therapy improvement

PDT is a form of photochemotherapy that involves the use of light, photosensitizers and oxygen. Basically, photosensitizers absorb light energy of specific wavelengths and generate singlet oxygen (1O<sub>2</sub>) and ROS, such as superoxide anions (O<sup>2-</sup>), hydroxyl radicals (OH) and hydrogen

peroxide (H<sub>2</sub>O<sub>2</sub>), at the cost of surrounding oxygen in the tissue. The ROS are highly reactive and can cause protein oxidation and DNA damage to induce cell death. Traditional photosensitizers usually have poor solubility and selectivity toward tumor tissue. Besides, common activation is usually located in the UV and visible range which are mostly absorbed by tissue. Noble metal NPs-based drug delivery systems can overcome these limitations and greatly improve PDT. Photosensitizers coupled with noble metal NPs exhibit targeted accumulation in only tumor cells, leading to minimal normal tissue damage. Tunable near-infrared (NIR) absorption of noble metal NPs can adjust the activation of PDT into the NIR range, thereby leading to efficient tissue penetration. Kautzka et al. combined PDT and chemotherapy by developing a gold-loaded liposome-based drug delivery system with Rose Bengal (RB), a photosensitizer in PDT, and DOX. The bilayer liposomes loaded with AuNPs (3-5 nm) significantly enhanced ROS generation than liposomes loaded with RB alone under 532 nm light illumination. Gold-loaded liposomes with RB and DOX showed increased cytotoxicity to human colon adenocarcinoma cells (HCT116), and DOX release was controlled by light illumination [162].

Photothermal therapy (PTT) is another cancer treatment based on energy conversion from NIR light into heat and generation of heat for tumor ablation. AuNPs are excellent PTT agents due to their unique and tunable SPR absorption. By changing the shape, size, morphology and structure, AuNPs-based PTT can be tuned to NIR where light absorption by hemoglobin and water in tissue is minimized to achieve tumor disruption [163]. Compared with AuNPs, Au nanorods (ANRs) have stronger plasmonic properties owning to their two localized surface plasmon bands corresponding to longitudinal resonance and transverse resonance along the long and short axes of the ANRs, respectively. The transverse plasmon resonates at ~520 nm, while the longitudinal plasmon resonates in NIR depending on the ANR aspect ratio. Increased ANR aspect ratio induced

enhanced light scattering and red shifts of the longitudinal band <sup>[164,165]</sup>. Furthermore, the higher surface-to-volume ratio of AuNRs improved drug loading than AuNPs <sup>[166]</sup>. Like AuNPs, AgNPs can also convert photon energy to thermal energy via SPR. Besides, the thermal conductivity of silver is 429 Wm<sup>-1</sup> K<sup>-1</sup>, the highest among all metals. Chitosan-coated silver nanotriangles (Chit-AgNTs) served as a photothermal agent against human non-small lung cancer cells (NCI-H460). The NPs displayed a strong NIR resonance at 724 nm and generated hyperthermia to destruct cancer cells.

High atomic number and adsorption coefficient enabled AgNPs to serve as a contrast agent in X-ray imaging and track the distribution of therapeutic agents. Shi et al. exploited combined graphene oxide (GO) and AgNPs to develop a NIR-triggered drug delivery system for X-ray imaging-guided photothermal therapy. The release of DOX loaded on the NPs could be controlled by NIR radiation. X-ray imaging showed a whitening effect at the tumor sites after 3 h injection of GO@Ag-DOX-NGR, suggesting a great potential of AgNPs for bioimaging [167].

Traditional electrochemical therapy (EChT) is a relatively inexpensive clinical cancer treatment method, utilizing destructive electrolysis induced by low-voltage direct current (DC) passing through electrodes. Here the electrodes are inserted into the tumor to induce localized pH variations and ROS to kill the cancer cells. EChT is not selective, however. A DC electric field can cause ion segregation harmful to biological tissue. Recently, Gu et al. first combined PtNPs with an electronic current and conceptualized electrodynamic therapy (EDT) to improve the efficacy of cancer therapy. The EDT method efficiently treated cancer and killed large sized tumors (over 500 mm<sup>3</sup>) in vivo based on the electro-driven catalytic reaction of PtNPs under a square-wave alternating current (AC) (Figure 5C). The applied AC induced PtNPs-catalyzed water molecules to decompose in the presence of chloride ions on PtNPs, leading to cytotoxic

hydroxyl radicals and ROS production. In addition, the harmful electrolysis products generated during PtNPs-catalyzed dissociation reactions can be neutralized under AC. PtNPs and ROS-based therapeutics, such as PDT, are usually inefficient because the hypoxic tumor environment cannot provide enough oxygen for ROS generation. However, PtNPs-based EDT generated ROS via PtNPs-catalyzed water decomposition, showing increased efficiency in tumor treatment and a great potential in local ablation of solid tumors with diminishing side effects <sup>[168]</sup>.

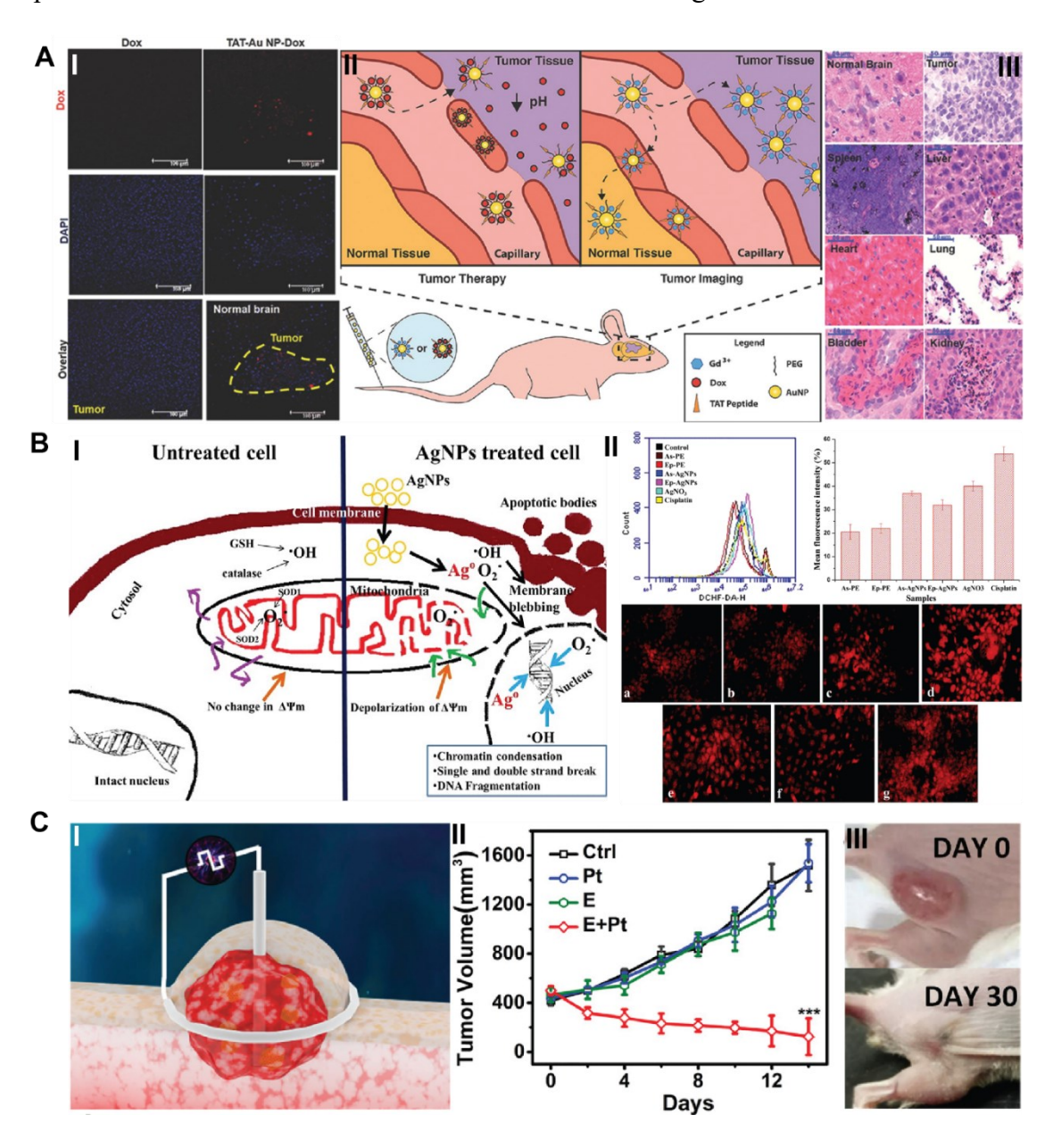


Figure 5. Tumor therapeutics with AuNPs, AgNPs and PtNPs. A. BBB penetration and tumor targeting of TAT-Au NP-DOX delivery in an intracranial U87 glioma mouse model. I) Confocal images of mouse brain tissues 24 h after I.V. injection showed DOX accumulation in a mouse brain after TAT-Au-NP injection. No DOX accumulation was observed when the free DOX was injected; II) Schematic illustrating the mechanism of AuNP-mediated therapeutic and diagnostic efficacy in brain tumors. III) Images of tissue samples with Haemotoxylin and Eosin (H&E) and silver enhancement staining from the TAT-AuNP-DOX-treated mice 6 weeks post injection [134]. Copyright 2014, John Wiley & Sons. B. Anticancer properties of AgNPs. I) Eclipta prostrata (Ep)/Alternanthera sessilis(As) synthesized AgNPs triggered ROS production in A431 skin carcinoma cells. II) In vitro ROS detection through flow cytometry and fluorescence microscopy after being treated with different agents, where PE means the respective plant extracts [158]. Copyright 2016, American Chemical Society. C. In vivo electrodynamic treatment showed that PtNPs combined with square-wave AC had the most effective tumor growth inhibition compared with AC or PtNPs treatment only. I) A scheme illustrating tumor treatment using wraparound electrodes. II) Average tumor volume growth curves of mice for four different treatment groups (n = 5 per group). III) Photographs of 4T1 tumor-bearing mice before and after EDT treatment with PtNPs for 30 days [168]. Copyright 2019, John Wiley & Sons.

#### 3.2 Porous silicon-based nanoparticles

Porous silicon-based NPs, mainly consisting of porous silicon NPs (PSiNPs) and mesoporous silica NPs (MSNs), have attracted much attention for applications in drug delivery, biosensing, cancer treatment and immunotherapy over the past decades [169]. Several remarkable structural and biomedical properties of PSiNPs and MSNs make them ideal materials for developing multifunctional drug delivery systems and cancer therapy platforms:

- (1) High surface-to-volume ratio. Porous structure provides a large surface area (up to 700-1000 m<sup>2</sup>/g) and a high pore volume (1cm<sup>3</sup>/g) [170], enabling improvement of drug loading.
- (2) Tunable porosity and pore size. The pore diameters of PSiNPs and MSNs can be precisely controlled to match the size of loaded molecules. Mesopores of 2-50 nm are most widely

- studied for drug delivery. In addition, MSNs possessing long-range ordered porous structure allow well-controlled drug loading and release [171].
- (3) Versatile surface modifications. The surfaces of PSiNPs and MSNs can be easily modified with various functional groups due to the presence of silanol groups on the pore surfaces, which provide further interaction points with adsorbed molecules or drugs and allow the design of multifunctional drug delivery systems with controllable site specific targeting, drug loading, particle stability and drug release [172].
- (4) Excellent biocompatibility and tunable biodegradability. The degradation of PSiNPs involves oxidation of Si to SiO and hydrolysis of Si-O bonds to orthosilicic acid (Si(OH)4) that is nontoxic to the human body and can be filtered by the kidney [173]. The degradation kinetics can be precisely controlled through structural design and surface modification.

Taken together, the above advantages warrant broad applications of PSiNPs in biomedicine and biomaterials research. In the next section, we focus on the utilities of PSiNPs and MSNs for enhanced cancer drug delivery and cancer therapy.

#### 3.2.1 Porous silicon-based nanoparticles for hydrophobic drug delivery

The application of nanotechnology combining with porous materials, such as mesoporous carbon, porous alumina and porous titanium, has been recognized as a most effective method to overcome the poor solubility and biocompatibility of many anticancer drugs <sup>[174]</sup>. PSiNPs and MSNs are the most commonly used nanomaterials to help improve drug solubility and bioavailability. Spatial confinement of porous structures can help reduce drug particle size, a key parameter influencing the solubility of drugs and maintaining drugs in a non-crystalline state. Wang et al. developed a core-shell mesoporous silica NP (csMSN)-based nanodrug delivery system to increase the

dissolution of paclitaxel (PAC) and improve its anticancer effect on human lung cancer. In vitro drug dissolution assay revealed that cumulative dissolution of PAC was 85.68 ±2.585% at 1 h for PAC-csMSN, comparison with the dissolution rate of 27.83 ± 3.724% for nonconjugated PAC powder. The IC<sub>50</sub> value of PAC-csMSN (30.74 ± 5.175 ng/ml) were four-time lower than that of PAC group (125.9 ± 3.762 ng/ml), indicating improved PAC absorption in the lungs to promote apoptosis by PAC-csMSN [175]. Nasab et al. used MSNs capped with a pH-sensitive biopolymer (CS-MCM-41) to enhance the transport of curcumin and investigated its anticancer property against U87MG glioblastoma cancer cell line. The higher toxicity of CS-MCM-41 than free curcumin indicated enhanced accumulation of curcumin in cancer cells [176].

Celecoxib (CEL) is a nonsteroidal anti-inflammatory drug (NSAID) commonly used for the treatment of pain and inflammation caused by osteoarthritis, juvenile arthritis, rheumatoid arthritis and ankylosing spondylitis. CEL has been regarded as a promising drug for cancer treatment but its application is limited to model drug research due to poor water solubility. Zhu et al. incorporated CEL into the pores of 3D face-centered cubic mesoporous silica (FMS) to develop a delivery system, and investigated the effect of pore size (16.0, 6.9, and 3.7 nm) on the dissolution rate in vitro. The dissolution rate of CEL form FMS gradually increased as the pore size increased due to increased escape of CEL from pores of larger sizes [177]. Similarly, Sahika et al. investigated the loading and release of CEL on SBA-15 mesoporous silica with surface functions of APTES grafted SBA-15-A and boron doped SBA-15-B particles. The loading of CEL increased in hexane because the nonpolar solvent did not compete with the highly hydrophobic drug. The drug release ability was found to be influenced by pH - more acidic CEL was increasingly soluble in an alkaline medium [178].

# 3.2.2 Surface modification to enhance targeting and drug release of porous silicon-based nanoparticles

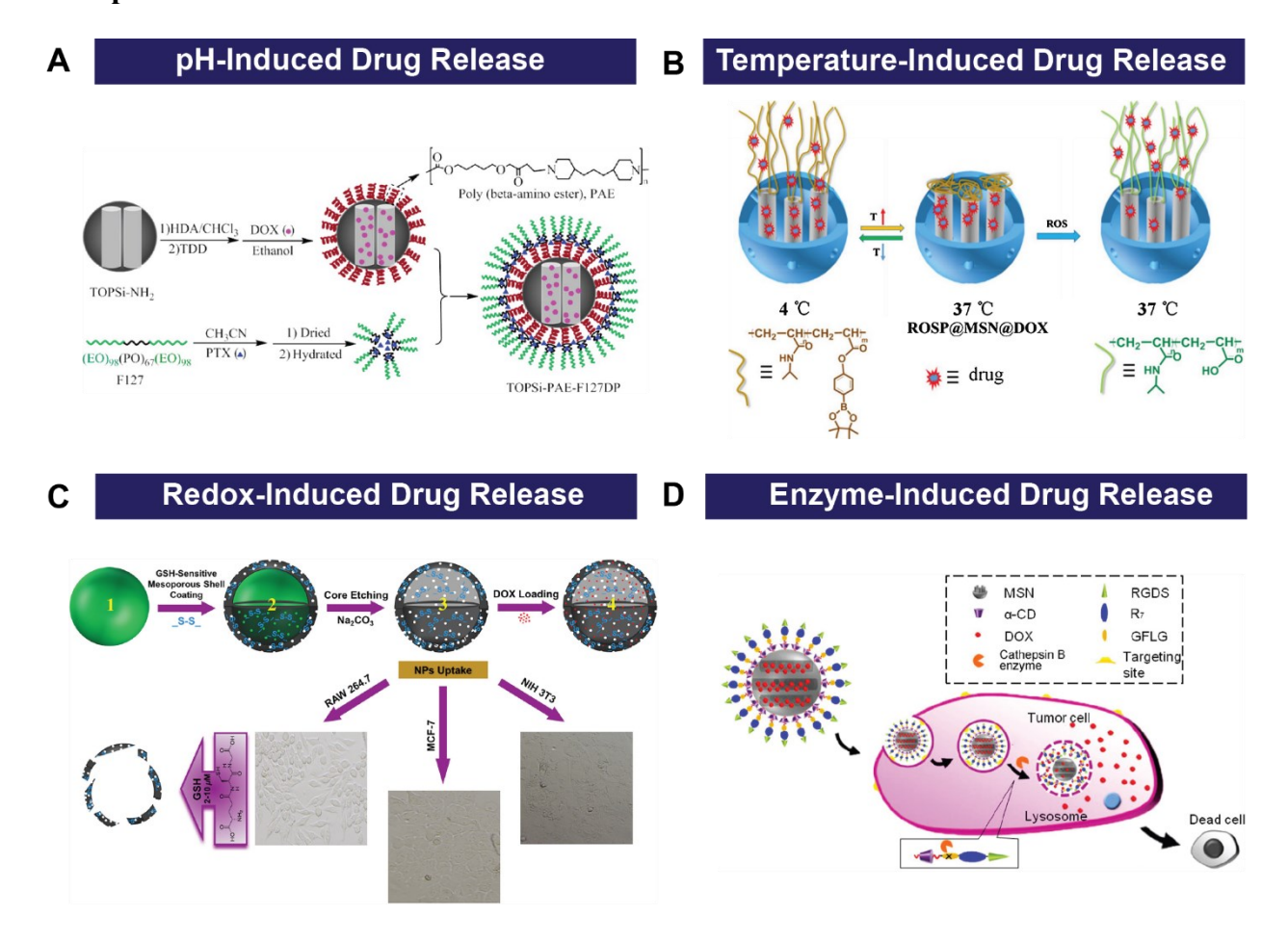


**Figure 6. Different drug release mechanisms of porous silicon-based NPs.** A. pH-induced drug release due to a pH-sensitive polymer <sup>[179]</sup>. Copyright 2018, Elsevier. B. Schematic of the behavior of dual-responsive NPs in aqueous medium <sup>[180]</sup>. Copyright 2015, American Chemical Society. C. Schematic representation of GSH-sensitive HMSiO<sub>2</sub> NPs <sup>[181]</sup>. Copyright 2018, Elsevier. D. Schematic representation of enzyme-induced MSNs <sup>[182]</sup>. Copyright 2015, American Chemical Society.

Although drug release can be modulated by changing the pore size, pore volume and particle shape of nanocarriers, much effort has been spent on achieving controllable drug delivery to target site by PSiNPs and MSNs via gate keepers. The gates keep loaded particles inside the pores and only open upon the stimuli of pH, temperature, redox and enzymes. Xu et al. constructed a pH-controlled multidrug delivery system containing DOX and PTX. DOX was loaded into the core of

PSi coated with poly (beta-amino ester) (PAE), while PTX was encapsulated into the external layer of pluronic F-127 ((EO)98(PO)67(EO)98) coated on the surface of the PSi NPs. Under physiological conditions (pH 7.0), PTX was first released. After internalization of NPs by cancer cells in acidic microenvironments, DOX was released due to the pH sensitivity of PAE. Early released PTX sensitized the microenvironments to overcome the delivery barriers of DOX and improved the delivery efficacy. In addition, the pluronic F127 layer has been demonstrated to overcome drug resistance in cancer cells (Figure 6A) [179]. Yu et al. presented ROS-responsive drug delivery system ROSP@MSN based on 4-(4,4,5,5-tetramethyl-1,3,2-dioxaborolan-2-yl) benzyl acrylate modified polymers (ROSP) coated on silica NPs. With the highly temperature-sensitive copolymer, DOX was loaded rapidly as temperature increased, and locked inside the MSNs above the lower critical solution temperature (LCST). Upon the stimulus of H<sub>2</sub>O<sub>2</sub>, the hydrophobic H<sub>2</sub>O<sub>2</sub>responsive monomer in the copolymer backbone was oxidized into hydrophilic acrylate, causing the LCST of polymer to rise above 37 °C and DOX release from the pores of MSNs. The release of DOX was controllable by the amount of H<sub>2</sub>O<sub>2</sub> (**Figure 6B**) [180]. Similarly, Tamarov et al. chose PSiNPs coated with a thermal responsive NIPAm-based polymer as drug carriers. The polymer kept the loaded drugs inside the pores of PSi below LCST and released them when the nanocarriers were heated above its LCST. Infrared radiation (IR) and radiofrequency (RF) radiation were used to provide the heat and control the drug release [183].

Degradable SiO<sub>2</sub>NPs have also been investigated as drug delivery systems. Since the concentration of glutathione (GSH) in intracellular microenvironment is significantly higher than in extracellular fluids (~100-1,000 times), redox-responsive drug delivery systems incorporating the disulfide bond have been constructed based on GSH-induced S-S bond degradation. Moghaddam et al. investigated the DOX release profile of tunable glutathione GSH-sensitive

biodegradable hollow MSNs containing disulfide linkages (S-S) in the outer shells in MCF-7 cells. The NPs were degraded in the presence of intracellular GSH ( $\sim$ 10 mM) (**Figure 6C**) <sup>[181]</sup>. Cheng et al. designed a drug delivery carrier based on rotaxane-modified MSNs. Multifunctional rotaxanes on MSNs were fabricated by using alkoxysilane tether,  $\alpha$ -cyclodextrin ( $\alpha$ -CD) and multifunctional peptides. The conjugated oligopeptides were composed of three functional segments, including a cell-penetrating peptide of seven arginine (R7) sequence, an enzymecleavable peptide of GFLG, and a tumor-targeting peptide of RGDS. When incubating the DOX-loaded MSNs with tumor and normal cells, the multifunctional NPs targeted tumor cells via specific interaction between RGDS and integrin receptor  $\alpha$ v $\beta$ 3 overexpressed on tumor cells, followed by penetrating cell membranes with the aid of R7 sequence. Upon cellular uptake, drugloaded MSNs released encapsulated drug quickly due to the breakage of GFLG peptide cleaved by cathepsin B, thereby resulting in an enhanced antitumor activity (**Figure 6D**) <sup>[182]</sup>.

#### 3.3 Magnetic iron oxide nanoparticles

Magnetic iron oxide NPs have been extensively studied for drug delivery and cancer therapy due to their unique magnetic property and excellent biocompatibility. Tumor targeting strategies based on the magnetic response of iron oxide NPs under a magnetic field has been widely attempted. Recently, there has been an increased focus on drug repurposing and magnetic-enhanced therapeutic efficiency, as reviewed in the section after.

#### 3.3.1 Magnetic iron oxide nanoparticles for drug repurposing

Artemisinin (ART), an endoperoxide-containing lactone isolated from artemisinin annua, has been widely used to treat human malaria. In recent years, the potential antitumor properties of ART and

its derivatives, such as dihydroartemisinin (DHA), artemether (ATM), arteether, artemisone, artesunate (AS) and artesunate (AS), have been verified. Repurposing ART and its analogs to cancer treatment has become an emerging area of focus. Fe<sup>2+</sup>-associated cleavage of the endoperoxide bridge (R-OO-R') contributes to the cytotoxicity and anti-cancer properties of ART due to the generation of ROS and other cytotoxic free radicals based on Fenton reactions, wherein Fe<sup>2+</sup>/Fe<sup>3+</sup> catalyzes disproportionation of H<sub>2</sub>O<sub>2</sub> and increases oxygen radical species. No apparent side effects like drug resistance have been observed for ART, an advantage over conventional chemotherapy drugs. However, the clinical application of ART has been greatly hampered due to its poor water solubility and fast metabolism. Furthermore, iron-induced cleavage of endoperoxide requires a large amount of Fe<sup>2+</sup> while Fe<sup>2+</sup> in cancer cells is deficient. Thus, simultaneous delivery of ART and Fe<sup>2+</sup> into cancer cells may be an effective strategy for enhancing the anti-cancer capacity of ART. Chen et al. developed a composite platform with Fe<sub>3</sub>O<sub>4</sub> nanocrystals as the core and mesoporous silica as the shell for ART delivery, and investigated the anti-cancer effect of ART against HeLa cells. Iron oxide NPs were degraded in acid environments after being internalized by HeLa cells, releasing Fe<sup>2+</sup> to non-enzymatically cleave the endoperoxide bridges of ART and kill tumor cells via ROS generation [184]. Ding et al. loaded ART on porous iron oxide magnetic superparticles (MSP). After accumulated at the tumor sites in a weakly acidic microenvironment, the magnetic core of MSP@ART@P nanodrug dissolved and released Fe<sup>2+</sup>. To verify the effect of Fe<sup>2+</sup> on the cytotoxicity of ART, MSP was replaced by mesoporous SiO<sub>2</sub> (MSNs) and no cytotoxicity of ART-loaded MSNs was measured, indicating that the Fe2+ generated from MSP played a key role in the anti-cancer property of ART [185]. Gao et al. synthesized ART-coupled magnetic liposomes encapsulated with Fe<sub>3</sub>O<sub>4</sub> NPs and cisplatin (cRGDAFePt@NPs) for high drug loading and better synergy. The Fe<sup>2+/</sup>Fe<sup>3+</sup> released from Fe<sub>3</sub>O<sub>4</sub>

NPs in acid lysosomes not only activated Fe-dependent ART but also sensitized cisplatin via catalyzing H<sub>2</sub>O<sub>2</sub> induced by cisplatin, leading to a significantly enhanced anticancer efficiency <sup>[195]</sup>. Zhang et al. used mesoporous Fe<sub>3</sub>O<sub>4</sub> for ART delivery, where HA coated on the NPs markedly avoided their aggregation and improved tumor targeting. When HA-mFe<sub>3</sub>O<sub>4</sub>/ART reached the tumor sites, pH-responsive bonds broke to simultaneously release Fe<sup>2+</sup> and ART <sup>[187]</sup>. Similarly, Wang et al. reported the ferrous ion-dependent cytotoxicity of DHA (**Figure 7A**). Novel Fe<sub>3</sub>O<sub>4</sub>@C@MIL-100(Fe) (FCM) NPs (MIL=Materials of Institute Lavoisier)) were developed to synchronously deliver DHA and Fe (III) in HeLa cells. The outer MIL-100(Fe) layer containing abundant Fe (III) rendered a pH-responsive degradation to release DHA and Fe (III), which was subsequently reduced to ferrous ions to react with DHA and ultimately led to bursts of intracellular ROS and enhanced DHA cytotoxicity. In addition, the antitumor effects of the nanoconstructs were enhanced by an externally applied magnetic field (**Figure 7B**) <sup>[188]</sup>.

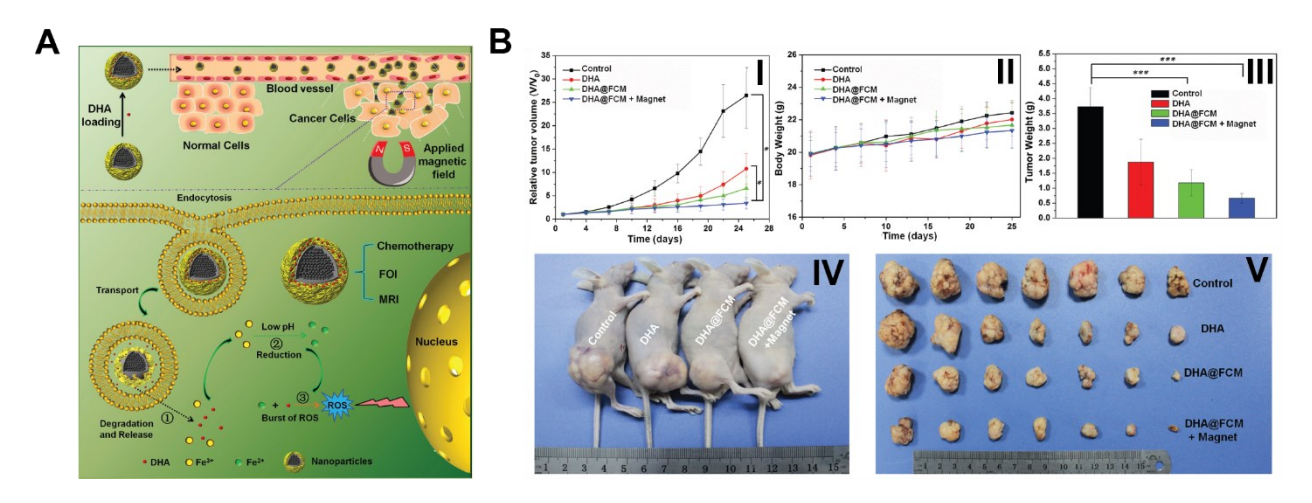


Figure 7. Magnetic iron oxide nanoparticles for drug repurposing. A. Schematic of tumor cell targeting of DHA-loaded FCM NPs assisted by an external magnetic field and the anticancer mechanism of the DHA delivery by intravenously injection of DHA@FCM. B. Tumor inhibition ratio of the corresponding group (I), body weights of mice for varied time periods for 25 days after the different treatment (II), weights of dissected tumor tissues 25 days after treatment (III), photograph of mice selected from each group randomly 25 days after treatment (IV), and excised tumors from different mice groups 25 days after treatments (V) [188]. Copyright 2016, Elsevier.

## 3.3.2 Magnetic iron oxide nanoparticles-enhanced cancer therapy

## (1) PTT therapy

Compared with conventional therapeutic approaches, PTT provides more precise spatial-temporal selectivity by controlling its NIR light source and improving tumor targeting to minimize normal tissue damage. To improve PTT efficacy, phototherapeutic agents used in PTT should have high photothermal energy conversion, low toxicity and high tumor targeting capacity. It is desirable to combine PTT with a noninvasive imaging technique, such as fluorescence (FL) or MRI, to directly monitor the location and distribution of phototherapeutic agents at tumor sites. Superparamagnetic iron oxide NPs (Fe<sub>3</sub>O<sub>4</sub> NPs) have been widely explored in PTT due to their low toxicity to healthy tissues and capacity in in vivo MRI.

To perform PTT in mice bearing C6 glioblastoma, Wang et al. constructed magnetic Fe<sub>3</sub>O<sub>4</sub> NP cores covered by a fluorescent carbon shell (~3.4 nm). The resultant BFNPs enabled dual FL bioimaging and MRI. Fe<sub>3</sub>O<sub>4</sub> NPs in BFNPs provided a contrast enhancement for T2-weighted MRI in vivo, while the fluorescent carbon shell gave rise to confocal fluorescence signal. In addition, the strong NIR absorption of BFNPs enabled efficient conversion of NIR light energy to heat and served as phototherapeutic agents to PTT for tumor treatment <sup>[189]</sup>. Chen et al. noted that highly crystallized iron oxide NPs (HCIONPs) showed a significantly enhanced PTT efficiency than commercial magnetic NPs due to the former's preferred lattice plane orientations. A 885 nm diode laser was employed to treat SUM-159 cancer cells at a power of 2.5 W cm<sup>-2</sup>, inducing complete tumor regression without relapse over a three-month period. In addition, the injected NPs were cleared via urinary excretion, thereby avoiding long-term toxicity.

# (2) PDT therapy

PDT involves light-responsive photosensitizers which interact with molecular oxygen and generate toxic ROS after exposure to light of specific wavelengths. However, tumor hypoxia in imperfect vascular system usually cannot provide enough O<sub>2</sub> for ROS production, thereby hampering PDT efficacy. As mentioned above, Fenton reaction can serve as a novel platform to enhance the ROS generation and improve PDT efficacy. Mesoporous Fe<sub>3</sub>O<sub>4</sub> NPs can constantly release Fe<sup>2+</sup> and interact with ART to generate significant amount of ROS. Moreover, due to the alternating magnetic field (AMF)—heat transfer characteristics of mFe<sub>3</sub>O<sub>4</sub>NPs, AMF irradiation could enhance the antitumor activity of particles by converting electromagnetic waves into heat and promoting ROS generation to enhance PDT [187]. Therapeutic agents delivered by magnetic NPs can be controlled by an external magnetic field (MF) applied to the tumor, inducing enhanced drug accumulation in targeted tumor regions for improved cancer therapy. Indeed, Li et al. used magnetic-responsive PEG-coated iron oxide nanoclusters (IONCs) to deliver a therapeutic agent chlorin e6 (Ce6). IONC—PEG—Ce6 shifted the excitation peak of Ce6 to NIR region, allowing for enhanced NIR adsorption and PDT effects [190].

# (3) Magnetic hyperthermia therapy (MHT)

Conventional hyperthermia aims to raise the temperature of tumor tissue to 40–43 °C for cancer cell destruction <sup>[191]</sup>. However, damage to healthy tissue is inevitable. Magnetic hyperthermia (MHT) is a promising method to overcome this issue due to its ease in tumor targeting. Magnetic NPs can convert magnetic energy to thermal energy upon exposure to an external alternating magnetic field (AMF). Espinosa et al. combined MHT and PTT to achieve a better therapy using iron oxide nanocubes. Iron oxide nanocubes displayed significantly increased heat generation

under a moderate laser power (0.3 W cm<sup>-2</sup>) and an AFM (520 kHz, 25 Mt) <sup>[192]</sup>. Compared with light or infrared radiation, the penetration depth of low frequency alternating magnetic field was much higher, inducing much deeper tissue destruction <sup>[193,194]</sup>.

# 4. Metal-Organic Nanoparticle Drug Delivery

#### 4.1 Introduction

The prior sections have reviewed the therapeutic potentials of soft materials and noble-metal NPs. Both classes of nanocarriers have been extensively used for drug delivery. Metal-organic hybrid materials, in comparison, are less explored systems. Historically, metal-organic interaction has been a concern in biopharmaceutics and formulation design. For example, the poorly soluble complex formed by calcium ions and tetracycline antibiotics is known to affect the drug absorption and reduce their bioavailability.

Recently, metal-organic NPs (MONs) have received increased attention as drug delivery systems. These hybrid materials are formed through complexation between metal ions and organic ligands. Several different terms have been used in literature to describe this type of materials, including metal-organic framework (MOF) [195], metal-organic nanodrug complex [196], coordination polymer [197], coordination complex [198], and nano metal-organic framework (NanoMOF) [199], among others. Metal ions function as an electron acceptor and form coordination with ligands containing electron donors (e.g., N, O and S). MOFs are supramolecular frameworks synthesized using ligands with multiple bonding points. However, ligands with a single bonding point have also been used; in this case, the metal/ligand complex may further assemble into NPs through non-coordination bonds such as hydrophobic interaction, hydrogen bonding, and others.

Despite minor differences, MONs have demonstrated unique advantages for drug delivery and share common features: (1) A variety of metal ions and organic ligands can be selected to prepare MONs of diverse structure, size, morphology and surface properties. The physicochemical properties of MONs can be fine-tuned for controlled drug release and targeted drug delivery. The large surface area of MONs, porous MOFs in particular, can provide a high drug loading capacity. MONs are superior to many other porous solids such as mesoporous silica, which suffers from low drug loading capacity and premature drug release. Also, the drug release profile of MONs can be adjusted by modifying drug-carrier interaction or by controlling the degradation of the MONs; (2) Many MONs are biodegradable materials due to the relatively weak bonding between metal ions and ligands. The selection of biocompatible building blocks (i.e. ligands and metal ions) and appropriate synthesis methods can further improve the biocompatibility of MONs; the latter will address safety concerns and pave the way for biomedical applications; (3) The flexibility in the design of MONs allows construction of multifunctional delivery systems with additional functional components, including tumor targeting ligands, imaging agents, etc.

Unlike the polymeric delivery carriers which usually possess no pharmacological effects, MONs will not only serve as "insert" delivery carriers but also function as active therapeutic agents. Bioactive MONs can be designed in several ways: (1) Metal ions may have an anticancer efficacy. The metal-organic complex prepared with pharmacologically active metal ions can be used as an anticancer agent. A good example is the platinum-based complexes. Many organic ligands have been used to complex with platinum and generated multiple anticancer agents including cisplatin, carboplatin, oxaliplatin, among others; (2) Many metal-organic complexes have been prepared by using active drug molecules as organic ligands. A high drug loading capacity can be achieved since the active drug is a part of the metal-organic complex. It can also provide extended drug release.

For example, bisphosphonate drugs have been used to prepare calcium-bisphosphate complexes <sup>[200–202]</sup>; (3) The complex formation may lead to enhanced pharmacological performance through synergistic effects. For example, copper dithiocarbamate has demonstrated a significantly better anticancer effect than its precursors (i.e., copper ion or dithiocarbamate) <sup>[203]</sup>.

## 4.2 Delivery of anticancer drugs and repurposed drugs with MONs

As a novel delivery system MONs have been explored for the delivery of anticancer drugs such as cisplatin <sup>[204,205]</sup>, paclitaxel <sup>[205,206]</sup>, dihydroartemisinin <sup>[188]</sup>, artemisinin <sup>[207]</sup>, doxorubicin and fluorouracil. Here we review MONs used for delivering representative chemotherapy drugs (e.g., doxorubicin, fluorouracil) and repurposed drugs (e.g., disulfiram, bisphosphonate, metformin and curcumin).

## (1) Chemotherapy drugs

## I. Doxorubicin

MONs of different compositions have been explored as delivery systems of DOX, through the high affinity of DOX with metal ions as well as other interactions of DOX with organic ligands. MONs composed of multiple different metal ions and ligands were studied by several research groups. For example, Horcajada et al. synthesized porous iron(III)-based metal—organic frameworks as nanoscale delivery systems for DOX and other drugs [208]. The use of MONs can overcome some common issues associated with traditional nanocarriers such as poor drug loading efficiency and rapid drug release.

Many DOX-loaded MONs demonstrate pH-sensitive drug release, showing minimal drug leakage at pH 7.4 and rapid drug release in acidic tumor environments. PAA@ZIF-8 was prepared by assembling ZIF-8 frameworks on the surface of polyacrylic acid NPs. DOX was loaded after

the MON synthesis [209]. DOX was also encapsulated with a "one-pot" process, in which drugs were loaded during the MON synthesis. For this method, DOX was dispersed within ZIF crystals [210]. A similar method was used to prepare Fe- and Zn-based MOFs with 1,3,5-Benzenetricarboxylic acid (H3 BTC) as the organic ligand for DOX delivery. Since DOX was dispersed within the MOF crystals, the drug loading was independent of MOF surface properties. Also, the release of DOX from Fe-BTC was slower than from Zn-BTC, mainly due to the stronger binding affinity between DOX and Fe-BTC than with ZN-BTC [211]. pH-sensitive DOX-loaded MONs could also be synthesized by mechanically grinding Gadolinium(III)-based MOFs [212]. A dual pH- and redox-sensitive DOX delivery system was synthesized through the surface modification of nanoscale MOF MIL-101. Because of the presence of a pH-sensitive benzoic imine bond and a redox sensitive disulfide bond, drug release was triggered by the acidic tumor environment and intracellular reducing environment [213]. The pH-sensitive delivery of DOX was also achieved with MONs with carboxylatopillar[5] arene switches [214], MIL-100(Al) metal organic gel [215], Cr<sup>3+</sup>-based metal-organic gel [216], AS1411 aptamer modified ZIF-8 [217], BSA/DOX coated with a MOF shell [218] and a Fe(bbi) system [219].

The release of DOX from MONs can be induced by other tumor-specific triggers. ATP-responsive hydrogel coated UiO-68 MONs (composed of Zr ions and amino triphenyl dicarboxylic acid) released drugs in response to high levels of ATP in tumor cells (**Figure 8**) <sup>[220]</sup>. In another study, UiO-68 MONs were modified with nucleic acids containing a sequence complementary to microRNA-21 or microRNA-221 over-expressed in cancer cells. These microRNAs in the cancer cells displaced nucleic acids on the surfaces of MONs and led to the release of DOX <sup>[221]</sup>. Similarly, with surface modified with a VEGF-specific aptamer, MONs released DOX triggered by VEGF overexpressed in tumor cells <sup>[222]</sup>.

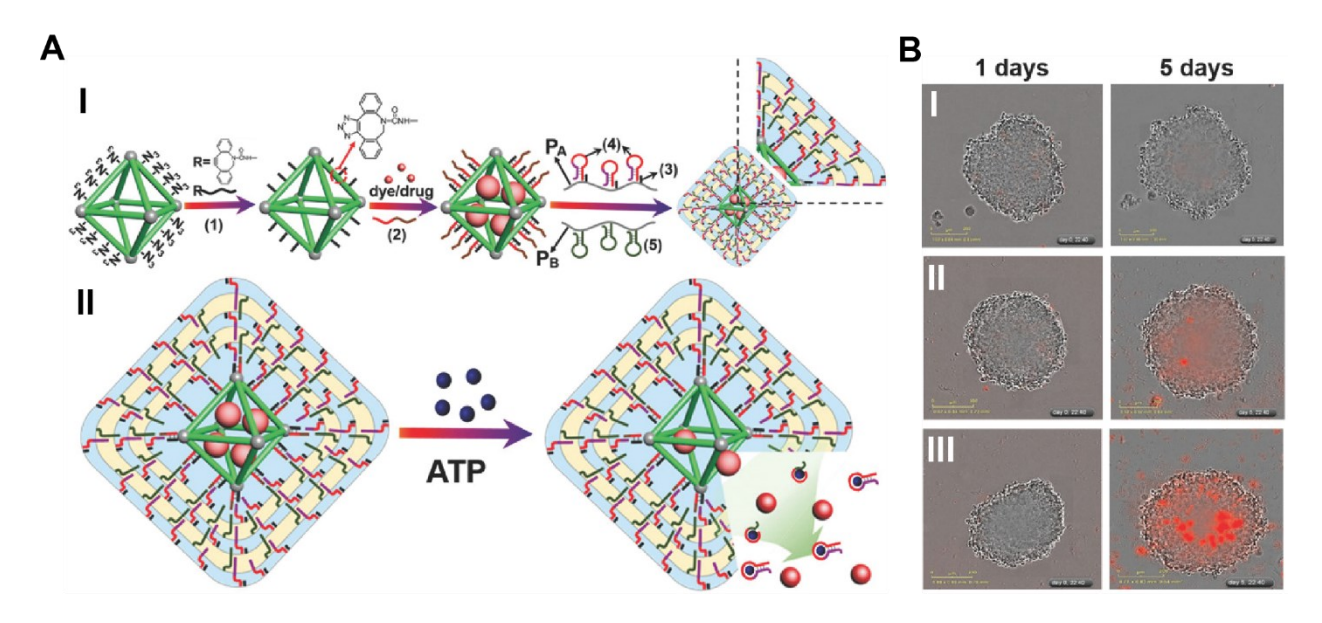


Figure 8. Stimuli-responsive nucleic acid-based polyacrylamide hydrogel-coated metal-organic framework nanoparticles for controlled release of DOX. A. I) Synthesis of ATP-responsive DNA/polyacrylamide-hydrogel-coated NMOFs loaded with a dye or DOX. II) Schematic mechanism to unlock the hydrogel-coated NMOFs and release the load via the formation of ATP-aptamer complexes. B. Representative phase-contrast and fluorescence images showed cell apoptosis after being treated with I) unloaded hydrogel-coated NMOFs, II) DOX-loaded NMOFs capped with (1)/(2) duplex units, and III) cells treated with DOX-loaded hydrogel-coated NMOFs [220]. Copyright 2017, John Wiley & Sons.

Multifunctional MONs have been designed for DOX delivery. Zhao et al. synthesized UiO-66 MONs containing Fe<sub>3</sub>O<sub>4</sub> as a theranostic agent for cancer diagnosis and treatment. The Fe<sub>3</sub>O<sub>4</sub> core served as a MRI contrast agent and DOX was loaded onto the UiO-66 MOF assembled on the surface of the Fe<sub>3</sub>O<sub>4</sub> core through the coordination interaction between DOX and the Zr(iv) centers of UiO-66 <sup>[223]</sup>. Bian et al. used MOF NPs of a triple modal imaging capability (e.g., fluorescence imaging, magnetic resonance, X-ray) for delivering DOX for cancer diagnosis and treatment <sup>[224]</sup>. ZIF-8 MONs coated onto gold nanorods were used for photo-thermal and chemotherapy, where the release of DOX was triggered by pH and NIR light. In addition, NIR irradiation as a photo-thermal therapy may have a synergistic effect with DOX chemotherapy <sup>[225]</sup>. Liu et al. synthesized a nanoscale zirconium-porphyrin MOF containing high contents of porphyrin

and DOX for imaging-guided chemotherapy and photodynamic therapy <sup>[226]</sup>. In another study, a DOX-loaded zirconium-based MOF was used for microwave thermal therapy <sup>[227]</sup>. MOFs have also been modified with tumor-targeting moieties including HA <sup>[228]</sup>, a mitochondria targeting molecule <sup>[227]</sup>, and folate <sup>[219]</sup>.

## II. Fluorouracil

Fluorouracil (FU) belongs to a family of chemotherapy drugs also known as anti-metabolites, which possess similar structures as endogenous molecules. The anticancer effects of FU rely on its ability to stop DNA replication and repair in cancer cells. FU has been used for treating breast cancer, colon cancer, stomach cancer, and others. Two zirconium-based MONs (e.g., MOF-808 and NH<sub>2</sub>-UiO-66) were explored as delivery systems for FU, where FU was attached to the surfaces of MONs through coordination interactions between the COOH groups of the FU molecules and Zr<sub>6</sub> clusters. Surface functionalization enhanced tumor cell uptake of MONs through active targeting [229]. [[Dy<sub>2</sub>(H<sub>2</sub>O)<sub>3</sub>(SDBA)<sub>3</sub>](DMA)<sub>6</sub>] were synthesized with 4,4'sulfonyldibenzoic acid (SDBA) and N,N-dimethylacetamide (DMA) using a solvothermal method. FU was loaded with a simple impregnation method [239]. Other MOFs used for the delivery of FU include MOFs synthesized with 3,5-bis((4'-carboxylbenzyl)-oxy)benzoic acid and N,Ndimethylformamide [231], metal-organic polyhedra prepared with a "click" chemistry [232], zincbased MOFs [233], Zn<sub>8</sub>(O)<sub>2</sub>(CDDB)<sub>6</sub>(DMF)<sub>4</sub>(H2O) microporous MOFs [234], zirconium-based MOFs with supramolecular gates [235,236], and engineered magnetic ZIF-90 NPs [237]. In another study, core-shell structured NPs composed of NaYF4:Yb<sup>3+</sup>, Er<sup>3+</sup> up-conversion NP core and ZIF-8 MOF shell was prepared. FU was loaded through absorption and was released in a pH-responsive manner. This NP can be used for cell imaging due to its luminescence property. Also, the surface modification with folate enhanced tumor targeting <sup>[238]</sup>. Gao et al. designed a multifunctional NP, Fe-MIL-53-NH<sub>2</sub>-FA-5-FAM/5-FU, through the post-synthesis modification of Fe-MIL-53-NH<sub>2</sub> MOF. It contained 5-FU as a drug, 5-carboxyfluorescein (5-FAM) as a fluorescence probe, FA as a tumor targeting agent, and Fe-MIL-53-NH<sub>2</sub> MOF as a magnetic contrast agent <sup>[239]</sup>. The same group also reported a similar delivery system, UIO-66-NH<sub>2</sub>-FA-5-FAM/5-F, which contained same functional components but a different MOF core <sup>[240]</sup>.

## (2) Repurposed drugs

## I. Disulfiram

Disulfiram (DSF) is an alcohol-aversion drug used for treating alcohol dependence for over sixty years. Recently, DSF has been repurposed as an anti-cancer agent and showed excellent anticancer activities in combination with copper ions (Cu<sup>2+</sup>). DSF/Cu can inhibit the proteasome/poly-Ub degradation pathway by targeting p97 segregase adaptor NPL4 <sup>[241–243]</sup>. The complex formed by copper and DDC, Cu(DDC)<sub>2</sub>, is a promising anticancer agent. Yet, it is challenging to develop a clinically useful formulation of Cu(DDC)<sub>2</sub> because of its poor water solubility. Recently, Metaplex technology or PRCosomes has been developed to prepare an injectable Cu(DDC)<sub>2</sub> liposome formulation with a high drug concentration and a loading efficiency <sup>[244,245]</sup>. However, the preparation of PRCosome involves complicated fabrication and purification, and is therefore problematic for large-scale manufacturing. Accordingly, Chen et al. developed a SMILE (stabilized metal ion ligand nanocomplex) technology to prepare Cu(DDC)<sub>2</sub> NPs <sup>[203]</sup>. In this method, aqueous solutions of copper ions and ligands (DDC) were rapidly mixed to form an insoluble Cu(DDC)<sub>2</sub> complex. The complex assembled into NPs stabilized by amphiphilic stabilizers such as 1, 2-distearoyl-sn-glycerol-3-phosphoethanolamine-poly(ethylene glycol) 2000

(DSPE-PEG), D-α-tocopherol polyethylene glycol 1000 succinate (TPGS), and methoxy poly(ethylene glycol) 5000 -b-poly(L-lactide) 5000 (PEG-PLA). The SMILE technology utilizes a simple formulation and a straightforward preparation process, thus can be easily scaled-up for mass production. The SMILE technology can prepare Cu(DDC)<sub>2</sub> NPs with a high drug concentration and has a great potential for clinical use. Cu(DDC)<sub>2</sub> NPs prepared with the SMILE technology demonstrated potent anticancer activities in different cancers, including drug resistant prostate cancers (**Figure 9A**).

## II. Bisphosphonate

Bisphosphonate drugs originally used for metabolic bone diseases have recently been repurposed for cancer treatment. For example, alendronate (ALN), an amino-bisphosphonate, has been widely used for osteoporosis, solid tumor bone metastases and myeloma bone disease. Alendronate was loaded into Zr-based MONs using the Zr-O cluster as the drug anchorage. The synthesized AL-MONs showed more efficient inhibition of cancer cells than free drugs [246]. Li et al. developed a method to prepare zoledronic acid-calcium complex NPs with a reverse microemulsion method. They systemically investigated the influence of different formulation and process parameters such as surfactant, reaction time and temperature, ratio as well as nature of the oil phase and water phase. They further incorporated the zoledronate-calcium complex into DSPE-PEG NPs. This NP formulation showed enhanced delivery of drugs into orthotropic mammary tumors [200,201]. The same group also loaded zoledronate-calcium NPs into PLGA NPs, further functionalized with octadecanoic acid-hydrazine-polyethylene glycol (2000). This delivery system showed a minimal burst release of zoledronate, enhanced toxicity in cancer cells as well as macrophages. In vivo experiments showed that this NP formulation reduced drug accumulation in bone, enhanced tumor targeting, and had a

better anticancer efficacy than free drugs [202]. In another study, calcium bisphosphonate NPs were synthesized to deplete tumor-associated macrophages and enhance cancer radiotherapy (Figure **9B**) <sup>[247]</sup>. Briefly, calcium bisphosphonate NPs were prepared with a water-in-oil emulsion method. Then, the NPs further modified 1,2-dihexadecanoyl-sn-glycerol-3were with phosphocholine(DPPC), cholesterol and 1,2-distearoyl-sn-glycerol-3-phosphoethanolamine-N-(methoxy(polyethylene glycol)-5000). Both 99mTC and 32P were incorporated into this NP system for bioimaging and radiotherapy. The bisphosphonate NPs effectively inhibited angiogenesis, promoted normalization of tumor vasculature, and improved the radiotherapy efficacy. Au et al. prepared calcium zoledronate MONs containing folate. This system demonstrated more potent anticancer activities than free zoledronate [248].

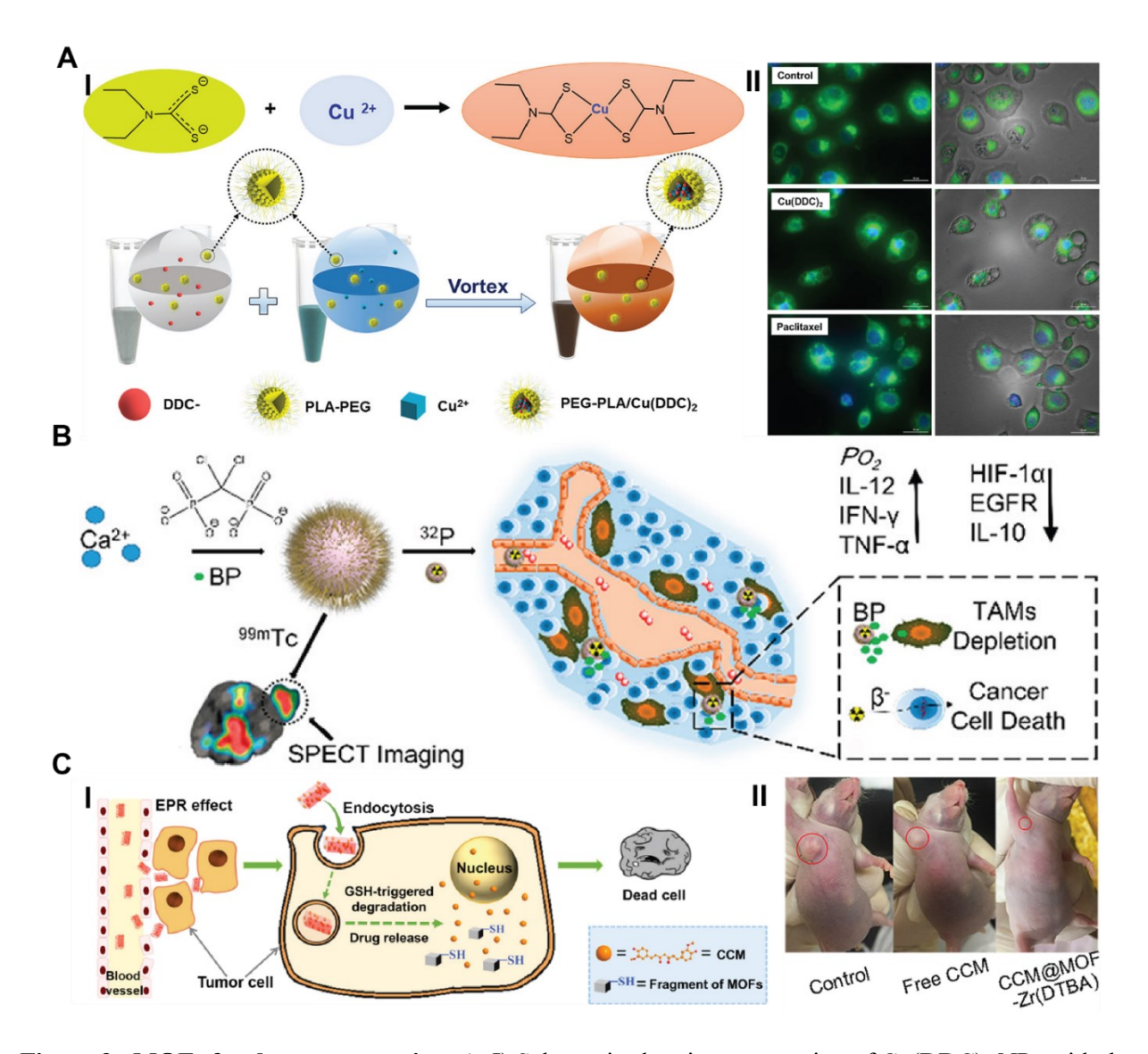


Figure 9. MOFs for drug repurposing. A. I) Schematic showing preparation of Cu(DDC)<sub>2</sub> NPs with the SMILE Technology. II) Treatment of Cu(DDC)<sub>2</sub> NPs induced formation of cytoplasmic vacuoles and cell paraptosis <sup>[203]</sup>. Copyright 2018, American Chemical Society. B. Scheme illustrating the 99mTc radiolabeling of CaBP-PEG NPs for tracing the in vivo fate of the NPs and CaBP(32P)-PEG NPs for synergistic combination radioisotope therapy with tumor-associated macrophages depletion <sup>[247]</sup>. Copyright 2018, American Chemical Society. C. Curcumin (CCM)-loaded redox-responsive metal–organic framework nanocarriers for anticancer drug delivery. I) Schematic of redox-responsive degradation of CCM@MOF-M(DTBA) in tumor cells for cancer therapy. In vivo antitumor efficiency of CCM@MOF-Zr(DTBA) in mice bearing HeLa xenograft tumors. II) Digital photographs of mice after 14 days of treatment with saline (control), free CCM, and CCM@MOF-Zr(DTBA) <sup>[249]</sup>. Copyright 2018, American Chemical Society.

#### III. Metformin

Metformin has been approved by the FDA for treating diabetes since 1994. Recent studies showed its potential as an anticancer agent. Metformin prolonged the survival of patients with different types of cancers [250]. A recent study explored the delivery of metformin with MOFs [251]. In this study, MOF was synthesized by using iron(III) chloride as the metal ion and trimesic acid (1,3,5-benzene tricarboxylic acid, BTC) as an organic linker. Metformin was incorporated as a building block of this MOF via its interaction with metal ions. Furthermore, the MOF surface was modified with sodium alginate to reduce premature drug release in acidic environments. When the formulation was administrated orally, drug release at stomach at an acidic pH was minimized. At small intestine, the alginate coating was expanded in response to the pH (>7), followed by drug release. This formulation improved oral bioavailability and reduced potential adverse effects of metformin.

## IV. Curcumin

Curcumin has demonstrated activities on several different signaling pathways such as the nuclear factor k-light-chain-enhancer of activated B cells (NF-κB) and transforming growth factor-β (TGF-β) pathways <sup>[252]</sup>. Due to poor water solubility and low bioavailability, there is a need for appropriate formulations to enhance curcumin delivery. Several research groups recently investigated the use of MONs for curcumin delivery <sup>[249,253]</sup>. Lei et al. prepared a curcumin-loaded redox-responsive MONs for cancer treatment. They used 4,4′-dithiobisbenzoic acid (4,4′-DTBA) as the organic ligand which could be cleaved by glutathione (GSH) overexpressed in tumor cells and facilitate curcumin release at tumor cells <sup>[249]</sup>(Figure 9C). Laha et al. developed FA-conjugated curcumin-loaded nanoscale MONs (IRMOF-3) as a targeted delivery system for treating triple-negative breast cancer cells <sup>[253]</sup>. This NP formulation induced cell apoptosis through the upregulation of BAX and the

inhibition of Bcl-2. In vivo study also showed that it effectively inhibited tumor growth and prolonged survival of mice.

# 4.3 Strategies for effectively loading drugs into MONs

MONs have been used as carriers for delivering therapeutic agents including small molecules, proteins, peptides and nucleic acids <sup>[254–256]</sup>. Herein, we will discuss strategies for effective drug loading into MONs.

## (1) Interactions to facilitate drug loading

Drugs can be loaded into MONs through various non-covalent interactions such as coordination bond, cation exchange and hydrogen bonding. Most drugs are loaded into MONs through coordination between the drug molecules and metal ions. The metal ions of MOFs function as Lewis acids (electron acceptors) and form strong interactions with molecules having electron donors (e.g., O, N and S). Drug molecules with phosphate groups (e.g., cidofovir, azidothimidine triphosphate) were loaded into MOF-100 (Fe), through the interaction between Fe and phosphate groups [208]. The zinc-DOX coordination bond and electrostatic interaction played a significant role in enhancing drug loading of polyacrylic acid@ZIF-8 NPs [209]. Procainamide HCl was loaded into porous zinc—adeninate MOFs through cation exchange [257]. Paclitaxel was encapsulated into MOFs through a hydrophobic interaction [206]. Ibuprofen was loaded into MIL-52 (Fe) through a hydrogen bond between the hydroxyl groups of MIL-53 (Fe) and the carboxylic acid group of ibuprofen [258]. Drugs can also be loaded through a synergistic effect of multiple interactions. For example, DOX was loaded into a ZIF-8 MOF through a combination of the coordination bond with zinc ions and the  $\pi$ - $\pi$  interaction with 2-methylimidazole ligand [217].

## (2) Different methods for drug loading

## I. In situ drug loading

In this method, drugs are mixed with metal ions or ligands prior to metal/ligand complexation. The MON formation and drug loading occur simultaneously. Many porous MOFs have tunable structures such as pores, channels and cavities. These porous structures on the surfaces of MONs cater for effective loading of drug cargos through different noncovalent interactions. Molecules of different properties have been successfully loaded into MONs via this method [254,255,259-265]. Since drugs are loaded through noncovalent interactions, the burst release is a major drawback. Efforts have been made to prevent the drug burst release issue and develop MONs with stimulated drug release properties. Tan et al. designed carboxylatopillar[5]arene-based supramolecular gates to prevent premature drug release from nanoUiO-66-NH<sub>2</sub> MOFs <sup>[235]</sup>. They also used a similar strategy to prepare zirconium MOFs, in which drug release was triggered by Ca<sup>2+</sup>, pH and temperature [236]. In another study, Meng et al. prepared zirconium MOFs bearing photo-responsive azobenzene groups to control drug release. The drug-loaded MOFs were surface-capped by βcyclodextrin through its binding with azobenzene. UV light caused conformational change in azobenzene groups, dissociation of  $\beta$ -cyclodextrin and drug release <sup>[266]</sup>. Post-synthesis treatments were also used to reduce the burst release of drugs from MONs. Orellana-Tavra et al. treated Zrbased MOF UiO-66 with a ball mill to convert the crystal form of the MOF into the amorphous form. The amorphous MOF demonstrated an extended release of a model drug, calcein, for more than one month. In contrast, the crystal form MOF with the same composition showed a quick drug release for only two days [267]. This research group also developed partial pore collapsed MOFs by thermal treatment to effectively reduce premature burst release and prolong the release time [268].

# II. Post-fabrication drug loading

Drug molecules can also be loaded into pre-formed MONs. This method minimizes interference with the MON formation process. Usually, drugs are loaded through non-covalent interactions such as coordination bond, hydrogen bond, electrostatic and hydrophobic interactions. Three sites at MONs can be potentially utilized for drug loading: functional sites in organic ligands, ligand defects within metal nodes, and coordinately unsaturated metal sites. Wettke et al. successfully loaded a variety of molecules bearing a His-tag into MOF utilizing the metal-histidine coordination bond (Figure 10) [269]. His-tag modified macromolecules were loaded onto three MOFs: MIL-88A, Zr-fum and HKUST-1 (Cu). The binding affinity of the cargos was affected by the length of the His-tag, environmental pH, as well as the types of metal nodes. Many recombinant proteins with His-tags are available, thus this method can be broadly applied. In addition to non-covalent binding through metal nodes, drug molecules can also be loaded through chemical conjugation with functional groups available on organic ligands. Taylor-Pashow et al. modified the Fe-based frameworks (MIL-101) with 2-amino terephthalic acids which provided functional groups for the conjugation of a BODIPY dye and a cisplatin prodrug. Conjugated drugs were released upon the degradation of the MONs [204].

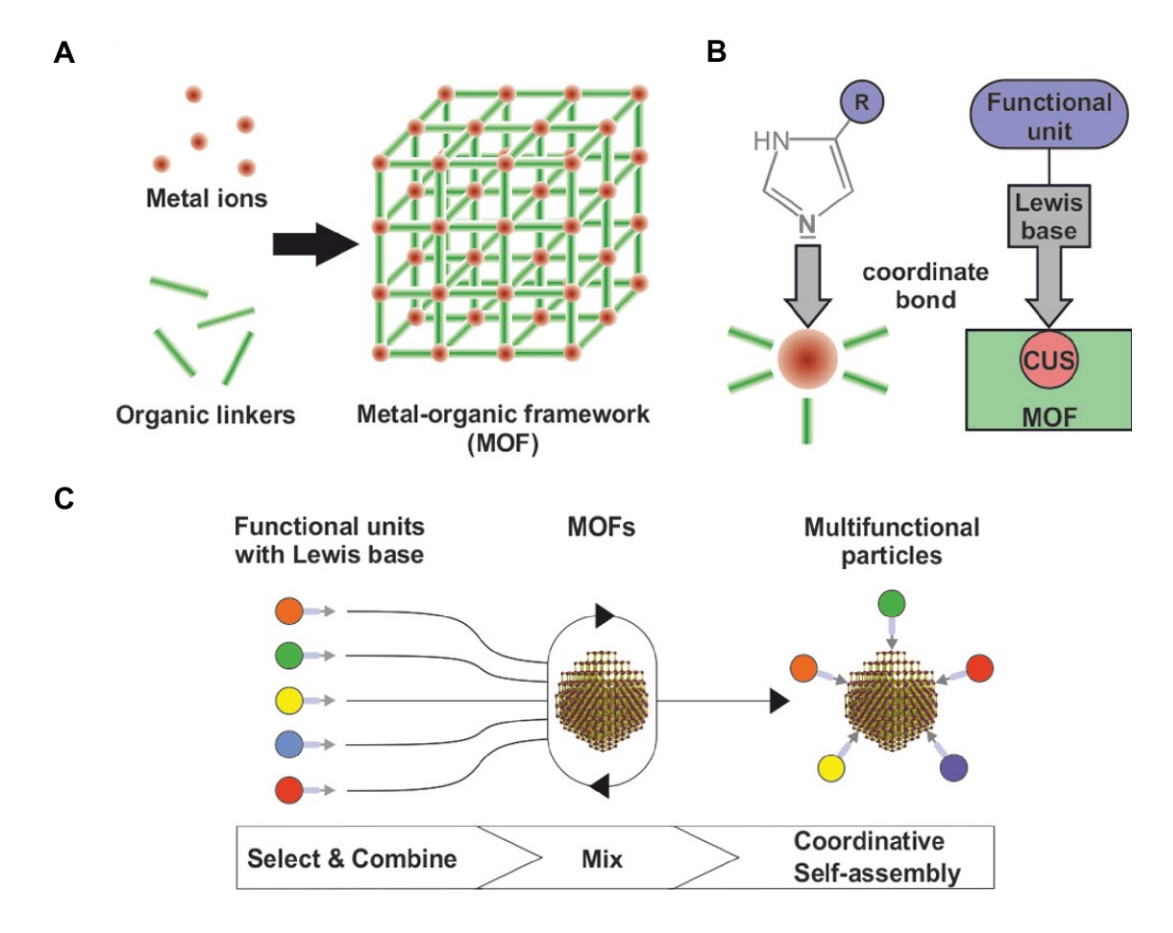


Figure 10. Coordinative self-assembly of His-tagged molecules with MOF NPs. A. molecular composition of MOFs; B. coordinative bond between the imidazole group of histidines acting as Lewis base and coordinatively unsaturated metal sites (CUS) acting as Lewis acid; C. multifunctional MOF NPs generated by coordinative attachment of functional units via self-assembly [269]. Copyright 2017, American Chemical Society.

Table 2. A summary of condensed nanoparticles reviewed for therapeutic applications.

Nanoparticles Dendrimer	Features  Three-dimensional geometric pattern with repeated branches and terminal functional group  Aqueous solubility Biodegradability	<ul> <li>Advanced Therapeutic Applications</li> <li>Improvement of drug stability</li> <li>Cancer imaging</li> <li>Antiangiogenic efficacy</li> <li>Tumor-targeted delivery</li> </ul>
Protein/DNA nanocage	<ul> <li>High drug-loading capacity</li> <li>Biodegradability</li> <li>Great stability</li> </ul>	<ul> <li>Tumor-targeted drug delivery</li> <li>Smart drug release platforms</li> <li>Blood-brain barrier (BBB) penetration</li> <li>Prolong half-life of drug</li> <li>Cancer imaging</li> </ul>
Nanohydrogel	<ul> <li>Hydrophilic polymer-crosslinked 3D structures</li> <li>Biocompatibility</li> <li>Biodegradability</li> <li>Swell and dissolve in water</li> </ul>	<ul> <li>Tumor-targeted drug delivery</li> <li>Smart drug release platforms</li> </ul>

Gold	<ul> <li>Facile surface modification</li> <li>Great biocompatibility</li> <li>Tunable near-infrared (NIR) absorption</li> <li>Enhanced permeability and retention (EPR) effect</li> </ul>	•	Photothermal therapy Photodynamic therapy Surface plasmon resonance (SPR) Blood-brain barrier (BBB) penetration
Silver	<ul> <li>Antimicrobial, anti-inflammatory, antibacterial, antifungal, antiangiogenetic, and anticancer activities</li> </ul>	•	Photothermal therapy Photodynamic therapy X-ray Imaging Angiogenesis therapy
Platinum	<ul> <li>Great catalysis properties</li> <li>Antioxidant effects</li> <li>Anti-cancer activity</li> </ul>	•	Anticancer-drug development Hadron therapy Electrodynamic therapy
Silicon/Silica	<ul> <li>High surface-to-volume ratio</li> <li>Tunable porosity and pore size.</li> <li>Versatile surface modifications</li> <li>Excellent biocompatibility and tunable biodegradability</li> </ul>	•	Poorly soluble drugs delivery Surface modification-enhanced tumor targeting
Iron oxide	<ul> <li>High surface-to-volume ratio</li> <li>Tunable porosity and pore size.</li> <li>Versatile surface modifications</li> <li>Excellent biocompatibility and tunable biodegradability</li> </ul>	•	Magnetic Hyperthermia Therapy Magnetic Resonance Imaging (MRI)
Metal-organic	<ul> <li>Hybrid structures</li> <li>Wide sources of synthetic materials</li> <li>Flexible structure and property design</li> <li>Controllable degradation</li> <li>Anticancer efficacy of metal ions</li> </ul>	•	Tumor-target drug delivery Drug repurposing Smart drug release platforms

# **5. Conclusions and Perspectives**

Drug repurposing has now emerged as a widely accepted and efficient method to accelerate new anticancer drug development. Although repurposed drugs or reformulated drug still need to be approved by the regulatory agencies, the drug repurpose strategy has several advantages. First, the safety profile of approved drugs has been extensively tested therefore, and therefore the use of these drug for different indication is less likely to fail due to the toxicity. Second, most of the preclinical studies, pharmacokinetics, biopharmaceutics studies and toxicity have been performed in prior studies. This could significantly save R&D cost and shorten the product development time [11]. The most successful example of drug repurpose is thalidomide which was a withdrawn drug due to its association with birth

defects but was repurposed to treat multiple myeloma. Novel drug delivery systems could enhance drug delivery into tumors, achieve optimized therapeutic efficacy with negligible off-target effects. Therefore, novel drug products may be developed through reformulation of old drugs or failed drugs with high toxicity or other undesirable properties. Accordingly, we have performed a comparative review on a variety of novel NPs and NFs with unique structures and physicochemical properties as advanced therapeutics for cancer drug repurposing and delivery (Table 2). We have highlighted the impact of nanotechnology on the fulfillment of crucial aspects in anticancer drug repurposing and delivery in the following areas: (i) maximizing the drug efficacy with modulated bio-distribution and minimized side effects; (ii) extending existing anti-cancer drugs to other cancer indications; (iii) identifying the antitumor effects of historically non-anticancer drugs; (iv) providing different drug delivery formulations such as oral administration, injection and inhalation of existing chemotherapeutic agents; (v) multiple drug-loaded combinational formulation to enhance therapeutic efficacy.

Although significant progress has been made in NP and NF delivery in preclinical studies, several challenges remain for the development of next-generation NP-based "smart" drug delivery platforms. The physicochemical properties and biological behaviors of NPs such as biocompatibility and size/dose-dependent toxicity should be characterized comprehensively. In addition, in-depth understanding of the mechanisms of the interactions between NPs and their hosting biological systems (i.e., proteins, cells, serum, tissues and organs) is critically needed to improve tumor targeting and minimize undesired uptake by non-targeted organs. The large-scale production remains a significant challenge for the commercialization of NPs and NFs which requires complicated fabrication. Although many novel materials have been developed to enhance drug delivery, their clinical use is subjected to regulatory approval. To minimize the regulatory obstacle, it is preferred to use the FDA-approved generally recognized as safe (GRAS) excipients. It is challenging to receive substantial industry

investment to support the clinical trials of many re-purposed drugs which are off-patent. Novel formulations based intellectual properties will be critical for the development of repurposed cancer medicines. With increasing investment in cancer research and clarification of nanotechnology-specific medical regulations, NP- and NF-based drug delivery and repurposing will not only provide novel cancer therapeutics, but also overcome the shortcomings of conventional platforms to ultimately provide patients with safer and efficacious treatment options.

#### **Conflict of Interest**

The authors declare no conflict of interest.

# Acknowledgements

This work was partially supported by the National Science Foundation CBET 1701363 (P.C.), the National Institute of Health R35GM133795 (P.C.), and Auburn University Launch Innovation Grant (F.L.). The content is solely the responsibility of the authors and does not necessarily represent the official views of the National Science Foundation or the National Institutes of Health.

#### REFERENCES

- [1] F. Bray, J. Ferlay, I. Soerjomataram, R. L. Siegel, L. A. Torre, A. Jemal, *CA. Cancer J. Clin.* **2018**, *68*, 394.
- [2] R. L. Siegel, K. D. Miller, A. Jemal, CA. Cancer J. Clin. 2018, 68, 7.
- [3] C. Xu, F. Haque, D. L. Jasinski, D. W. Binzel, D. Shu, P. Guo, Cancer Lett. 2018, 414, 57.
- [4] D. Bovelli, G. Plataniotis, F. Roila, Ann. Oncol. 2010, 21, 277.
- [5] C. Holohan, S. Van Schaeybroeck, D. B. Longley, P. G. Johnston, Nat. Rev. Cancer 2013, 13, 714.
- [6] E. Ruoslahti, S. N. Bhatia, M. J. Sailor, J. Cell Biol. 2010, 188, 759.
- [7] O. M. Kutova, E. L. Guryev, E. A. Sokolova, R. Alzeibak, I. V Balalaeva, *Cancers (Basel)*. **2019**, 11, 68.
- [8] W. Lee, C. Loo, M. Ghadiri, C. Leong, P. M. Young, D. Traini, *Adv. Drug Deliv. Rev.* **2018**, *133*, 107.
- [9] S. C. Gupta, B. Sung, S. Prasad, L. J. Webb, B. B. Aggarwal, *Trends Pharmacol. Sci.* **2013**, *34*, 508.
- [10] J. J. Hernandez, M. Pryszlak, L. Smith, C. Yanchus, N. Kurji, V. M. Shahani, S. V. Molinski, *Front. Oncol.* **2017**, *7*, 273.
- [11] S. Pushpakom, F. Iorio, P. A. Eyers, K. J. Escott, S. Hopper, A. Wells, A. Doig, T. Guilliams, J. Latimer, C. McNamee, A. Norris, P. Sanseau, C. David, P. Munir, *Nat. Rev. Drug Discov.* **2018**, *18*, 41.
- [12] K. Park, S. Lee, E. Kang, K. Kim, K. Choi, I. C. Kwon, Adv. Funct. Mater. 2009, 19, 1553.
- [13] A. K. Biswas, M. R. Islam, Z. S. Choudhury, A. Mostafa, M. F. Kadir, *Adv. Nat. Sci. Nanosci. Nanotechnol.* **2014**, *5*, 043001.
- [14] Y. Liu, H. Miyoshi, M. Nakamura, Int. J. Cancer 2007, 120, 2527.
- [15] E. Boisselier, D. Astruc, Chem. Soc. Rev 2009, 38, 1759.
- [16] X. Xu, W. Ho, X. Zhang, N. Bertrand, O. Farokhzad, *Trends Mol. Med.* **2015**, *21*, 223.
- [17] Y. Zhou, Z. Peng, E. S. Seven, R. M. Leblanc, J. Control. Release 2018, 270, 290.
- [18] J. Shi, P. W. Kantoff, R. Wooster, O. C. Farokhzad, Nat. Rev. Cancer 2017, 17, 20.
- [19] L. Brannon-peppas, J. O. Blanchette, Adv. Drug Deliv. Rev. 2012, 64, 206.
- [20] I. Brigger, C. Dubernet, P. Couvreur, Adv. Drug Deliv. Rev. 2012, 64, 24.
- [21] D. Peer, J. M. Karp, S. Hong, O. C. Farokhzad, R. Margalit, R. Langer, *Nat. Nanotechnol.* **2007**, *2*, 751.
- [22] P. Singh, S. Pandit, V. R. S. S. Mokkapati, A. Garg, V. Ravikumar, I. Mijakovic, *Int. J. Mol. Sci.* **2018**, *19*, DOI 10.3390/ijms19071979.
- [23] F. Caruso, T. Hyeon, V. Rotello, J. I. Zink, Chem. Soc. Rev 2012, 41, 2590.
- [24] D. Bobo, K. J. Robinson, J. Islam, K. J. Thurecht, S. R. Corrie, *Pharm. Res.* **2016**, *33*, 2373.
- [25] P. Horcajada, R. Gref, T. Baati, P. K. Allan, G. Maurin, P. Couvreur, Chem. Rev. 2012, 112, 1232.
- [26] T. Cedervall, I. Lynch, S. Lindman, T. Berggård, E. Thulin, H. Nilsson, K. A. Dawson, S. Linse, *Proc. Natl. Acad. Sci. U. S. A.* **2007**, *104*, 2050.
- [27] M. Lundqvist, J. Stigler, G. Elia, I. Lynch, T. Cedervall, K. A. Dawson, *Proc. Natl. Acad. Sci. U. S. A.* **2008**, *105*, 14265.
- [28] N. Bertrand, P. Grenier, M. Mahmoudi, E. M. Lima, E. A. Appel, F. Dormont, J. Lim, R. Karnik, R. Langer, O. C. Farokhzad, *Nat. Commun.* **2017**, *8*, 777.
- [29] T. P. Davis, P. Chun, M. Wang, I. Javed, J. Mater. Chem. B 2018, 6, 6026.
- [30] H. S. Choi, W. Liu, P. Misra, E. Tanaka, J. P. Zimmer, B. I. Ipe, M. G. Bawendi, J. V Frangioni, *Nat. Biotechnol.* **2007**, *25*, 1165.
- [31] P. Guo, D. Liu, K. Subramanyam, B. Wang, J. Yang, J. Huang, D. T. Auguste, M. A. Moses, *Nat. Commun.* **2018**, *9*, 130.
- [32] G. Bonacucina, M. Cespi, M. Misici-Falzi, G. F. Palmieri, J. Pharm. Sci. 2009, 98, 1.
- [33] P. G. De Gennes, H. Hervet, J. Phys., Lett. 1983, 44, 351.
- [34] S. Mignani, S. El Kazzouli, M. Bousmina, J. P. Majoral, Adv. Drug Deliv. Rev. 2013, 65, 1316.

- [35] J. R. Baker, ASH Education Program Book, **2009**, pp. 708–719.
- [36] S. Lo, A. Kumar, J. Hsieh, X. Sun, Mol. Pharm. 2013, 10, 793.
- [37] D. A. Tomalia, *Polym. J.* **1985**, *17*, 117.
- [38] C. J. Hawker, J. M. J. Fréchet, J. Am. Chem. Soc. 1990, 112, 7638.
- [39] T. Kawaguchi, K. L. Walker, C. L. Wilkins, J. S. Moore, J. Am. Chem. Soc. 1995, 117, 2159.
- [40] P. Wu, A. K. Feldman, A. K. Nugent, C. J. Hawker, A. Scheel, B. Voit, J. Pyun, J. M. J. Frechet, K. B. Sharpless, V. V. Fokin, *Angew. Chemie Int. Ed.* **2004**, *43*, 3928.
- [41] V. Maraval, J. Pyzowski, A. Caminade, J. Majoral, J. Org. Chem. 2003, 68, 6043.
- [42] M. Liu, K. Kono, J. M. J. Frechet, J. Control. Release 2000, 65, 121.
- [43] M. Liu, K. Kono, J. M. J. Fréchet, J. Polym. Sci. Part A Polym. Chem. 1999, 37, 3492.
- [44] S. Sanyakamdhorn, D. Agudelo, L. Bekale, H. A. Tajmir-Riahi, Colloids Surf., B 2016, 145, 55.
- [45] S. Sanyakamdhorn, L. Bekale, D. Agudelo, H. A. Tajmir-Riahi, *Colloids Surf., B* **2015**, *135*, 175.
- [46] Y. Cheng, Q. Wu, Y. Li, T. Xu, J. Phys. Chem. B 2008, 112, 8884.
- [47] L. P. Mendes, J. Pan, V. P. Torchilin, *Molecules* **2017**, *22*, 1.
- [48] S. Lalwani, A. Chouai, L. M. Perez, V. Santiago, S. Shaunak, E. E. Simanek, *Macromolecules* **2009**, *42*, 6723.
- [49] M. Markowicz, P. Szymański, M. Ciszewski, A. Kłys, E. Mikiciuk-Olasik, *J. Biol. Phys.* **2012**, *38*, 637
- [50] J. Hu, Y. Cheng, Y. Ma, Q. Wu, T. Xu, J. Phys. Chem. B 2009, 113, 64.
- [51] K. Yang, Y. Cheng, X. Feng, J. Zhang, Q. Wu, T. Xu, J. Phys. Chem. B 2010, 114, 7265.
- [52] M. A. Mintzer, M. W. Grinstaff, Chem. Soc. Rev. 2011, 40, 173.
- [53] N. Malik, E. G. Evagorou, R. Duncan, Anticancer. Drugs 1999, 10, 767.
- [54] O. L. P. De Jesu, H. R. Ihre, L. Gagne, J. M. J. Fre, F. C. Szoka, S. Francisco, *Bioconjug. Chem.* **2002**, *13*, 453.
- [55] C. Kojima, K. Kono, K. Maruyama, T. Takagishi, *Bioconjug. Chem.* **2000**, *11*, 910.
- [56] D. Bhadra, S. Bhadra, S. Jain, N. K. Jain, Int J Pharm. 2003, 257, 111.
- [57] E. M. . van den Berg, E. . Meijer, Angew. Chemie Int. Ed. English 1993, 32, 1308.
- [58] N. Shao, Y. Su, J. Hu, J. Zhang, H. Zhang, Y. Cheng, Int. J. Nanomedicine 2011, 6, 3361.
- [59] A. Szulc, L. Pulaski, D. Appelhans, B. Voit, B. Klajnert-maculewicz, *Int. J. Pharm.* **2016**, *513*, 572.
- [60] P. Garrigue, J. Tang, L. Ding, A. Bouhlel, A. Tintaru, E. Laurini, Y. Huang, Z. Lyu, M. Zhang, L.
  B. Samantha Fernandez, W. Lani, E. Masi, D. Marsone, Y. Weng, X. Liu, S. Giorgioc, J. Iovannai,
  S. Pricle, B. Guilleta, L. Peng, *Proc. Natl. Acad. Sci. U. S. A.* 2018, 115, 11454.
- [61] K. T. Al Jamal, S. Akerman, J. E. Podesta, A. Yilmazer, J. A. Turton, A. Bianco, N. Vargesson, C. Kanthou, A. T. Florence, G. M. Tozer, *Proc. Natl. Acad. Sci.* **2010**, *107*, 3966.
- [62] K. T. Al Jamal, W. Al Jamal, J. T. W. Wang, N. Rubio, J. Buddle, D. Gathercole, M. Zloh, K. Kostarelos, *ACS Nano* **2013**, *7*, 1905.
- [63] J. Bugno, H. Hsu, R. M. Pearson, H. Noh, S. Hong, Mol. Pharm. 2016, 13, 2155.
- [64] H. Li, J. Z. Du, J. Liu, X. Du, S. Shen, Y. Zhu, X. Wang, X. Ye, S. Nie, J. Wang, *ACS Nano* **2016**, *10*, 6753.
- [65] M. Labieniec-Watala, C. Watala, J. Pharm. Sci. 2015, 104, 2.
- [66] R. Jevprasesphant, J. Penny, R. Jalal, D. Attwood, N. B. McKeown, A. D'emanuele, *Int. J. Pharm.* **2003**, *252*, 263.
- [67] M. Hołota, J. Magiera, S. Michlewska, M. Kubczak, N. S. del Olmo, S. García-Gallego, P. Ortega, F. J. de la Mata, M. Ionov, M. Bryszewska, *Biomolecules* **2019**, *9*, 155.
- [68] D. Yang, Z. L. Ma Nwe Nwe Linn Oo, Gulam Roshan Deen, X. J. Loh, *Macromol. Rapid Commun.* **2017**, *38*, 1700410.
- [69] K. Khanna, S. Varshney, A. Kakkar, Polym. Chem. 2010, 1, 1171.
- [70] Y. K. Chong, I. Zainol, C. H. Ng, I. H. Ooi, J. Polym. Res. 2019, 26, 79.
- [71] P. Alonso-cristobal, M. Laurenti, F. J. Sanchez-muniz, E. López-cabarcos, J. Rubio-retama, *Polymer* **2012**, *53*, 4569.

- [72] T. Liu, W. Xue, B. Ke, M. Xie, D. Ma, *Biomaterials* **2014**, *35*, 3865.
- [73] G. Jutz, P. van Rijn, B. Santos Miranda, A. Böker, *Chem. Rev.* **2015**, *115*, 1653.
- [74] P. M. Harrison, P. Arosio, *Biochim. Biophys. Acta* **1996**, *1275*, 161.
- [75] L. Li, C. J. Fang, J. C. Ryan, E. C. Niemi, J. A. Lebrón, P. J. Björkman, H. Arase, F. M. Torti, S. V Torti, M. C. Nakamura, *Proc. Natl. Acad. Sci.* **2010**, *107*, 3505.
- [76] B. Chiou, E. Lucassen, M. Sather, A. Kallianpur, J. Connor, *Glia* **2018**, *66*, 1317.
- [77] L. Conti, S. Lanzardo, R. Ruiu, M. Cadenazzi, F. Cavallo, S. Aime, S. G. Crich, *Oncotarget* **2016**, 7, 66713.
- [78] R. Fan, S. W. Chew, V. V. Cheong, B. P. Orner, *Small* **2010**, *6*, 1483.
- [79] Z. Zhen, W. Tang, H. Chen, X. Lin, T. Todd, G. Wang, T. Cowger, X. Chen, J. Xie, *ACS Nano* **2013**, *7*, 4830.
- [80] E. Falvo, E. Tremante, A. Arcovito, M. Papi, N. Elad, A. Bo, V. Morea, G. Conti, G. To, G. Fracasso, P. Giacomini, P. Ceci, *Macromolecules* **2016**, *17*, 514.
- [81] M. Liang, K. Fan, M. Zhou, D. Duan, J. Zheng, D. Yang, J. Feng, X. Yan, *Proc. Natl. Acad. Sci.* **2014**, *111*, 14900.
- [82] R. K. Watt, BioMetals 2011, 24, 489.
- [83] T. Douglas, D. R. Ripoll, *Protein Sci.* **1998**, 7, 1083.
- [84] C. Wang, C. Zhang, Z. Li, S. Yin, Q. Wang, F. Guo, Y. Zhang, R. Yu, Y. Liu, Z. Su, *Biomacromolecules* **2018**, *19*, 773.
- [85] H. G. J. Alqaraghuli, S. Kashanian, R. Rafipour, K. Mansouri, *Artif. Cells, Nanomed., Biotechnol.* **2018**, *46*, S847.
- [86] L. Calisti, I. Benni, M. Cardoso, P. Baiocco, B. Ruzicka, A. Bof, E. Falvo, F. Malatesta, A. Bonamore, *Biochim. Biophys. Acta* **2016**, *1861*, 450.
- [87] S. Nowag, R. Haag, Angew. Chemie Int. Ed. 2014, 53, 49.
- [88] M. T. Calejo, S. A. Sande, B. Nyström, Expert Opin. Drug Deliv. 2013, 10, 1669.
- [89] B. Du, S. Jia, Q. Wang, X. Ding, Y. Liu, H. Yao, J. Zhou, Biomacromolecules 2018, 19, 1026.
- [90] C. Lin, M. Javadi, D. M. Belnap, J. R. Barrow, W. G. Pitt, *Nanomedicine: NBM* **2014**, *10*, 67.
- [91] E. Simsek, M. A. Kilic, J. Magn. Magn. Mater. 293 2005, 293, 509.
- [92] M. A. Kilic, E. Ozlu, S. Calis, J. Biomed. Nanotechnol. 2012, 8, 508.
- [93] Z. Chen, M. Zhai, X. Xie, Y. Zhang, S. Ma, Z. Li, F. Yu, B. Zhao, M. Zhang, Y. Yang, X. Mei, Mol. Pharm. 2017, 14, 3087.
- [94] X. Huang, J. Chisholm, J. Zhuang, Y. Xiao, G. Duncan, X. Chen, J. S. Suk, J. Hanes, *Proc. Natl. Acad. Sci.* **2017**, *114*, E6595.
- [95] S. Dostalova, Z. Heger, J. Kudr, M. Vaculovicova, V. Adam, M. Stiborova, T. Eckschlager, R. Kizek, in *Nano Based Drug Deliv. Zagerb IAPC Publ.*, **2015**, pp. 217–233.
- [96] M. Li, D. Wu, Y. Chen, G. Shan, Y. Liu, *Mater. Sci. Eng. C* **2019**, *95*, 11.
- [97] H. Li, W. Zhang, L. Ding, X. Li, Y. Wu, J. Tang, J. Biomater. Appl. 2019, 33, 1202.
- [98] C. Y. Lin, S. J. Yang, C. L. Peng, M. J. Shieh, ACS Appl Mater Interfaces 2018, 10, 6096.
- [99] A. F. Breen, G. Wells, L. Turyanska, T. D. Bradshaw, Cancer Rep. 2019, e1155.
- [100] R. Indra, T. Černá, Z. Heger, J. Hraběta, M. Wilhelm, S. Dostálová, A. Lengálová, M. Martínková, V. Adam, T. Eckschlager, H. H. Schmeiser, V. M. Arlt, M. Stiborová, *Toxicology* **2019**, *419*, 40.
- [101] K. Fan, C. Cao, Y. Pan, D. Lu, D. Yang, J. Feng, L. Song, M. Liang, X. Yan, *Nat. Nanotechnol.* **2012**, *7*, 459.
- [102] X. Lin, J. Xie, L. Zhu, S. Lee, G. Niu, Y. Ma, K. Kim, X. Chen, *Angew. Chemie Int. Ed.* **2011**, *50*, 1569.
- [103] T. Kitagawa, H. Kosuge, M. Uchida, M. M. Dua, Y. Iida, R. L. Dalman, T. Douglas, M. V McConnell, *Mol. Imaging Biol.* **2012**, *14*, 315.
- [104] C. Zhang, X. Li, C. Tian, G. Yu, Y. Li, W. Jiang, C. Mao, ACS Nano 2014, 8, 1130.
- [105] A. R. Chandrasekaran, O. Levchenko, Chem. Mater. 2016, 28, 5569.
- [106] A. S. Hoffman, P. S. Stayton, O. Press, N. Murthy, C. A. Lackey, C. Cheung, F. Black, J. Campbell, N. Fausto, T. R. Kyriakides, P. Bornstein, *Polym. Adv. Technol.* **2002**, *13*, 992.

- [107] Y. Kumashiro, K. M. Huh, T. Ooya, N. Yui, Biomacromolecules 2001, 2, 874.
- [108] P. M. de la Torre, S. Torrado, S. Torrado, Biomaterials 2003, 24, 1459.
- [109] Y. H. Bae, S. W. Kim, Adv. Drug Deliv. Rev. 1993, 11, 109.
- [110] A. Setia, P. Ahuja, in *Org. Mater. as Smart Nanocarriers Drug Deliv.*, William Andraw Publishing, **2018**, pp. 293–368.
- [111] S. Z. Nanogels, L. Circulation, L. S. Accumulation, ACS Nano 2012, 6, 6681.
- [112] T. B. Circulation, A. C. Anselmo, M. Zhang, S. Kumar, D. R. Vogus, S. Menegatti, M. E. Helgeson, S. Mitragotri, *ACS Nano* **2015**, *9*, 3169.
- [113] C. Gonçalves, P. Pereira, M. Gama, *Materials* **2010**, *3*, 1420.
- [114] T. B. Becher, M. C. P. Mendonça, M. A. de Farias, R. V Portugal, M. B. de Jesus, C. Ornelas, *ACS Appl. Mater. Interfaces* **2018**, *10*, 21891.
- [115] S. Deguchi, H. Otake, Y. Nakazawa, N. Hiramatsu, N. Yamamoto, N. Nagai, *Int. J. Mol. Sci.* **2017**, *18*, 2720.
- [116] N. Gupta, F. I. Al-Saikhan, B. Patel, J. Rashid, F. Ahsan, Int. J. Pharm. 2015, 488, 33.
- [117] A. Jaromin, R. Zarnowski, M. Piętka-Ottlik, D. R. Andes, J. Gubernator, *Nanomedicine* **2018**, *13*, 1139.
- [118] I. Mylonaki, F. Strano, S. Deglise, E. Allémann, F. Alonso, J.-M. Corpataux, C. Dubuis, J.-A. Haefliger, O. Jordan, F. Saucy, F. Delie, *J. Control. Release* **2016**, *232*, 93.
- [119] N. Nagai, C. Yoshioka, Y. Mano, W. Tnabe, Y. Ito, N. Okamoto, Y. Shimomura, *Exp. Eye Res.* **2015**, *132*, 115.
- [120] S. S. Rostamkalaei, J. Akbari, M. Saeedi, K. Morteza-Semnani, A. Nokhodchi, *Colloids Surf., B* **2019**, *175*, 150.
- [121] J. Wang, X. Hu, D. Xiang, Drug Deliv. 2018, 25, 1319.
- [122] R. R. Arvizo, S. Bhattacharyya, R. A. Kudgus, K. Giri, R. Bhattacharya, P. Mukherjee, *Chem. Soc. Rev.* **2012**, *41*, 2943.
- [123] Y. Xin, M. Yin, L. Zhao, F. Meng, L. Luo, cancer Biol. Med. 2017, 14, 228.
- [124] A. G. Tkachenko, H. Xie, D. Coleman, W. Glomm, J. Ryan, M. F. Anderson, S. Franzen, D. L. Feldheim, *J. Am. Chem. Soc.* **2003**, *125*, 4700.
- [125] K. J. Stine, Biochem. Insights **2017**, 10, 1.
- [126] J. R. Ashton Id, E. B. Gottlin, E. F. Patz, J. L. West, C. T. Badea, *PLoS One* **2018**, *13*, e0206950.
- [127] I. Ocsoy, B. Gulbakan, M. I. Shukoor, X. Xiong, T. Chen, D. H. Powell, W. Tan, *ACS Nano* **2013**, 7, 417.
- [128] L. A. Austin, M. A. Mackey, E. C. Dreaden, M. A. El, Arch. Toxicol. 2014, 88, 1391.
- [129] S. Eustis, M. A. El-Sayed, Chem. Soc. Rev. 2006, 35, 209.
- [130] H. Chugh, D. Sood, I. Chandra, V. Tomar, G. Dhawan, R. Chandra, *Artif. Cells, Nanomed., Biotechnol.* **2018**, *46*, 1210.
- [131] B. Klebowski, J. Depciuch, M. Parlinska-Wojtan, J. Baran, Int. J. Mol. Sci. 2018, 19, 4031.
- [132] S. Mukherjee, I. Mitra, V. P. Reddy B., C. Fouzder, S. Mukherjee, S. Ghosh, U. Chatterji, S. C. Moi, *J. Mol. Liq.* **2017**, *247*, 126.
- [133] H. Sonowal, P. B. Pal, J. J. Wen, S. Awasthi, K. V. Ramana, S. K. Srivastava, *Sci. Rep.* **2017**, 7, 3182.
- [134] Y. Cheng, Q. Dai, X. F. Ramin A. Morshed, D. A. W. Michelle L. Wegscheid, Y. Han, L. Zhang, B. Auffinger, A. L. Tobias, E. Rincón, B. Thaci, A. U. Ahmed, P. C. Warnke, C. He, M. S. Lesniak, *Small* 2014, 10, 5137.
- [135] A. B. Etame, C. A. Smith, W. C. W. Chan, J. T. Rutka, *Nanomedicine: NBM* **2011**, *7*, 992.
- [136] S. Dhar, E. M. Reddy, A. Shiras, V. Pokharkar, B. L. V Prasad, *Chem. A Eur. J.* **2008**, *14*, 10244.
- [137] C. Lee, H. Kim, J. Yu, S. Hwan, S. Ban, S. Oh, D. Jeong, J. Im, M. Jun, T. H. Kim, *Eur. J. Med. Chem.* **2017**, *142*, 416.
- [138] F. Benyettou, R. Rezgui, F. Ravaux, T. Jaber, K. Blumer, M. Jouiad, L. Motte, J. C. Olsen, C. Platas-Iglesias, M. Magzoub, A. Trabolsi, *J. Mater. Chem. B* **2015**, *3*, 7237.

- [139] Y. Octavia, C. G. Tocchetti, K. L. Gabrielson, S. Janssens, H. J. Crijns, A. L. Moens, *J. Mol. Cell. Cardiol.* **2012**, *52*, 1213.
- [140] Q. Yang, J. Peng, Y. Xiao, W. Li, L. Tan, X. Xu, Z. Qian, ACS Appl. Mater. Interfaces 2018, 10, 150.
- [141] F. Yusof, N. Akmal, S. Ismail, J. Appl. Pharm. Sci. 2015, 5, 140.
- [142] H. Hatcher, R. Planalp, J.Cho, F. M. Torti, S. V. Torti, Cell. Mol. Life Sci. 2008, 65, 1631.
- [143] M. Gera, N. Sharma, M. Ghosh, D. L. Huynh, S. J. Lee3, T. Min1, T. Kwon, J. D. Kee, *Oncotarget* **2017**, *8*, 66680.
- [144] S. Singh, B. B. Aggarwal, J. Biol. Chem. 1995, 270, 24995.
- [145] P. Khandelwal, A. Alam, A. Choksi, S. Chattopadhyay, P. Poddar, ACS Omega 2018, 3, 4776.
- [146] R. K. Gangwar, V. A. Dhumale, D. Kumari, U. T. Nakate, S. W. Gosavi, R. B. Sharma, S. N. Kale, S. Datar, *Mater. Sci. Eng. C* **2012**, *32*, 2659.
- [147] K. Sindhu, A. Rajaram, K. J. Sreeramc, R. Rajaram, RSC Adv. 2014, 4, 1808.
- [148] S. Garg, A. Garg, Int. J. Pharm. Sci. Res. 2018, 9, 1160.
- [149] M. A. Hamzawy, A. M. Abo-youssef, H. F. Salem, S. A. Mohammed, *Drug Deliv.* 2017, 24, 588.
- [150] S. Kim, J. E. Choi, J. Choi, K. H. Chung, K. Park, J. Yi, D. Ryu, *Toxicol. Vitr.* **2009**, *23*, 1076.
- [151] R. Foldbjerg, D. A. Dang, H. Autrup, Arch. Toxicol. 2011, 85, 743.
- [152] S. Gurunathan, J. W. Han, V. Eppakayala, M. Jeyaraj, J.-H. Kim, Biomed Res. Int. 2013, 2013.
- [153] T. Zhang, L. Wang, Q. Chen, C. Chen, Yonsei Med. J. 2014, 55, 283.
- [154] M. A. Franco-molina, E. Mendoza-gamboa, C. A. Sierra-rivera, R. A. Gómez-flores, P. Zapata-benavides, P. Castillo-tello, J. M. Alcocer-gonzález, D. F. Miranda-hernández, R. S. Tamez-guerra, C. Rodríguez-padilla, *J. Exp. Clin. Cancer Res.* **2010**, *29*, 148.
- [155] D. Guo, L. Zhu, Z. Huang, H. Zhou, Y. Ge, W. Ma, J. Wu, X. Zhang, X. Zhou, Y. Zhang, Y. Zhao, N. Gu, *Biomaterials* **2013**, *34*, 7884.
- [156] P. V Asharani, G. Low, K. Mun, M. P. Hande, S. Valiyaveettil, ACS Nano 2009, 3, 279.
- [157] M. Ovais, A. T. Khalil, A. Raza, M. A. Khan, I. Ahmad, N. U. Islam, M. Saravanan, M. F. Ubaid, M. Ali, Z. K. Shinwari, *Nanomedicine* **2016**, *12*, 3157.
- [158] D. Nayak, M. Kumari, S. Rajachandar, S. Ashe, N. C. Thathapudi, B. Nayak, *ACS Appl. Mater. Interfaces* **2016**, *8*, 28538.
- [159] A. Samadi, H. Klingberg, L. Jauffre, A. Kjær, P. Martin, L. B. Oddershede, *Nanoscale* **2018**, *10*, 9097.
- [160] H. Xia, F. Li, X. Hu, W. Park, S. Wang, Y. Jang, Y. Du, S. Baik, S. Cho, T. Kang, D.-H. Kim, D. Ling, K. M. Hui, T. Hyeon, ACS Cent. Sci. 2016, 2, 802.
- [161] M. S. Shoshan, T. Vonderach, B. Hattendorf, H. Wennemers, *Angew. Chemie Int. Ed.* **2019**, *58*, 4901.
- [162] Z. Kautzka, S. Clement, E. M. Goldys, W. Deng, Int. J. Nanomedicine 2017, 12, 969.
- [163] F. Emami, A. Banstola, A. Vatanara, S. Lee, J. O. Kim, J. H. Jeong, S. Yook, *Mol. Pharm.* 2019, 16, 1184.
- [164] L. Tong, Q. Wei, A. Wei, J.-X. Cheng, *Photochem. Photobiol.* **2009**, 85, 21.
- [165] K.-S. Lee, M. A. El-Sayed, J. Phys. Chem. B 2006, 110, 19220.
- [166] V. Mosquera, E. Villar-Alvarez, A. Cambón, A. Pardo, V. X. Mosquera, A. Bouzas-Mosquera, A. Topete, S. Barbosa, P. Taboada, *ACS Omega* **2018**, *3*, 12633.
- [167] J. Shi, L. Wang, J. Zhang, R. Ma, J. Gao, Y. Liu, C. Zhang, Z. Zhang, *Biomaterials* **2014**, *35*, 5847.
- [168] T. Gu, Y. Wang, Y. Lu, L. Cheng, L. Feng, H. Zhang, X. Li, G. Han, Z. Liu, *Adv. Mater.* **2019**, *31*, 1806803.
- [169] R. Narayan, U. Y. Nayak, A. M. Raichur, S. Garg, *Pharmaceutics* **2018**, *10*, 118.
- [170] R. R. Castillo, M. Vallet-regí, Expert Opin. Drug Deliv. 2017, 14, 229.
- [171] S. Jafari, H. Derakhshankhah, L. Alaei, A. Fattahi, Varnamkhastia, B. Shiri, A. A. Saboury, *Biomed. Pharmacother.* **2019**, *109*, 1100.
- [172] W. Li, Z. Liu, F. Fontana, Y. Ding, D. Liu, J. T. Hirvonen, H. A. Santos, Adv. Mater. 2018, 30,

- 1703740.
- [173] T. Tieu, M. Alba, R. Elnathan, A. Cifuentes-rius, N. H. Voelcker, Adv. Ther. 2019, 2, 1800095.
- [174] J. Riikonen, W. Xu, V. Lehto, Int. J. Pharm. 2018, 536, 178.
- [175] T. Wang, Y. Liu, C. Wu, Nanoscale Res. Lett. 2017, 12, 66.
- [176] N. A. Nasab, H. H. Kumleh, M. Beygzadeh, S. Teimourian, M. Kazemzad, *Artif. Cells, Nanomed., Biotechnol.* **2018**, *46*, 75.
- [177] W. Zhu, L. Wan, C. Zhang, Y. Gao, X. Zheng, T. Jiang, S. Wang, Mater. Sci. Eng. C 2014, 34, 78.
- [178] Z. S. Eren, S. Tunçer, G. Gezer, L. T. Yildirim, S. Banerjee, A. Yilmaz, *Microporous Mesoporous Mater.* **2016**, *235*, 211.
- [179] W. Xu, R. Thapa, D. Liu, T. Nissinen, S. Granroth, A. Närvänen, M. Suvanto, H. A. Santos, V. P. Lehto, *Mol. Pharm.* **2015**, *12*, 4038.
- [180] F. Yu, H. Wu, Y. Tang, Y. Xu, X. Qian, W. Zhu, Int. J. Pharm. 2018, 536, 11.
- [181] S. P. Hadipour Moghaddam, M. Yazdimamaghani, H. Ghandehari, *J. Control. Release* **2018**, *282*, 62.
- [182] Y. J. Cheng, G. F. Luo, J. Y. Zhu, X. D. Xu, X. Zeng, D. B. Cheng, Y. M. Li, Y. Wu, X. Z. Zhang, R. X. Zhuo, F. He, *ACS Appl. Mater. Interfaces* **2015**, *7*, 9078.
- [183] K. Tamarov, W. Xu, L. Osminkina, S. Zinovyev, P. Soininen, A. Kudryavtsev, M. Gongalsky, A. Gaydarova, A. Närvänen, V. Timoshenko, V. P. Lehto, *J. Control. Release* **2016**, *241*, 220.
- [184] J. Chen, Z. Guo, H. B. Wang, J. J. Zhou, W. J. Zhang, Q. W. Chen, *Biomaterials* **2014**, *35*, 6498.
- [185] Y. Ding, J. Wan, Z. Zhang, F. Wang, J. Guo, C. Wang, ACS Appl. Mater. Interfaces 2018, 10, 4439.
- [186] Z. Gao, Y. Li, C. You, K. Sun, P. An, C. Sun, M. Wang, X. Zhu, B. Sun, *ACS Appl. Bio Mater.* **2018**, *1*, 270.
- [187] H. Zhang, Q. Chen, X. Zhang, X. Zhu, J. Chen, H. Zhang, L. Hou, Z. Zhang, ACS Appl. Mater. Interfaces 2016, 8, 33484.
- [188] D. Wang, J. Zhou, R. Chen, R. Shi, G. Xia, S. Zhou, Z. Liu, N. Q. Zhang, H. Wang, Z. Guo, Q. Chen, *Biomaterials* **2016**, *107*, 88.
- [189] H. Wang, Q. Mu, R. Revia, K. Wang, B. Tian, G. Lin, W. Lee, Y.-K. Hong, M. Zhang, *J. Control. Release* **2018**, *289*, 70.
- [190] Z. Li, C. Wang, L. Cheng, H. Gong, S. Yin, Q. Gong, Y. Li, Z. Liu, *Biomaterials* 2013, 34, 9160.
- [191] A. Jordan, R. Scholz, P. Wust, H. Fa, R. Felix, J. Magn. Magn. Mater. 1999, 201, 413.
- [192] A. Espinosa, R. Di Corato, J. Kolosnjaj-Tabi, P. Flaud, T. Pellegrino, C. Wilhelm, *ACS Nano* **2016**, *10*, 2436.
- [193] N. A. Usov, M. S. Nesmeyanov, V. P. Tarasov, Sci. Rep. 2018, 8, 1224.
- [194] M. Saeed, W. Ren, A. Wu, Biomater. Sci. 2018, 6, 708.
- [195] L. Wang, L. Wang, Z. Xie, J. Mater. Chem. B 2018, 6, 707.
- [196] P. Zhang, J. Wang, H. Chen, L. Zhao, B. Chen, C. Chu, H. Liu, Z. Qin, J. Liu, Y. Tan, X. Chen, G. Liu, J. Am. Chem. Soc. **2018**, 140, 14980.
- [197] J. Zhao, Y. Yang, X. Han, C. Liang, J. Liu, X. Song, Z. Ge, Z. Liu, *ACS Appl Mater Interfaces* **2017**, *9*, 23555.
- [198] Z. Ma, B. Moulton, Coord. Chem. Rev. 2011, 255, 1623.
- [199] M. B. Majewski, H. Noh, T. Islamoglu, O. K. Farha, J. Mater. Chem. A 2018, 6, 7338.
- [200] X. Li, Y. W. Naguib, S. Valdes, S. Hufnagel, Z. Cui, ACS Appl Mater Interfaces 2017, 9, 14478.
- [201] X. Li, Y. W. Naguib, Z. Cui, Int J Pharm. 2017, 526, 69.
- [202] X. Li, S. A. Valdes, R. F. Alzhrani, S. Hufnagel, S. D. Hursting, Z. Cui, ACS Appl Mater Interfaces 2019, 11, 7311.
- [203] W. Chen, W. Yang, P. Chen, Y. Huang, F. Li, ACS Appl. Mater. Interfaces 2018, 10, 41118.
- [204] K. M. L. Taylor-Pashow, J. Della Rocca, Z. Xie, S. Tran, W. Lin, *J. Am. Chem. Soc.* **2009**, *131*, 14261.
- [205] M. Filippousi, S. Turner, K. Leus, P. I. Siafaka, E. D. Tseligka, M. Vandichel, S. G. Nanaki, I. S. Vizirianakis, D. N. Bikiaris, P. Van Der Voort, G. Van Tendeloo, *Int. J. Pharm.* **2016**, *509*, 208.

- [206] A. R. Chowdhuri, D. Bhattacharya, S. K. Sahu, *Dalt. Trans.* **2016**, *45*, 2963.
- [207] D. Wang, J. Zhou, R. Chen, R. Shi, G. Zhao, G. Xia, R. Li, Z. Liu, J. Tian, H. Wang, Z. Guo, H. Wang, Q. Chen, *Biomaterials* **2016**, *100*, 27.
- [208] P. Horcajada, T. Chalati, C. Serre, B. Gillet, C. Sebrie, T. Baati, J. F. Eubank, D. Heurtaux, P. Clayette, C. Kreuz, J. Chang, Y. K. Hwang, V. Marsaud, P. Bories, L. Cynober, S. Gil, G. Férey, P. Couvreur, R. Gref, *Nat. Mater.* **2009**, *9*, 172.
- [209] H. Ren, L. Zhang, J. An, T. Wang, L. Li, X. Si, L. He, X. Wu, C. Wang, Z. Su, *Chem. Commun.* **2014**, *50*, 1000.
- [210] H. Zheng, Y. Zhang, L. Liu, W. Wan, P. Guo, A. M. Nyström, X. Zou, *J. Am. Chem. Soc.* **2016**, 138, 962.
- [211] C. Adhikari, A. Chakraborty, *Chempluschem* **2016**, *17*, 1070.
- [212] T. Kundu, S. Mitra, P. Patra, A. Goswami, D. Díaz Díaz, R. Banerjee, *Chem. A Eur. J.* **2014**, *20*, 10514.
- [213] X. Wang, Z. Dong, H. Cheng, S. Wan, W. Chen, M. Zou, J. Huo, H. Deng, X. Zhang, *Nanoscale* **2015**, *7*, 16061.
- [214] L. Tan, H. Li, Y. Qiu, D. Chen, X. Wang, R. Pan, Y. Wang, S. X. Zhang, B. Wang, Y. Yang, *Chem. Sci.* **2015**, *6*, 1640.
- [215] Y. Feng, C. Wang, F. Ke, J. Zang, J. Zhu, Nanomaterials 2018, 8, 446.
- [216] N. Sharma, P. K. Sharma, Y. Singh, C. M. Nagaraja, ACS Omega 2019, 4, 1354.
- [217] K. Dong, Z. Wang, Y. Zhang, J. Ren, X. Qu, ACS Appl. Mater. Interfaces 2018, 10, 31998.
- [218] Z. Liang, Z. Yang, H. Yuan, C. Wang, J. Qi, K. Liu, R. Cao, H. Zheng, *Dalt. Trans.* **2018**, *47*, 10223.
- [219] P. F. Gao, L. L. Zheng, L. J. Liang, X. X. Yang, Y. F. Li, C. Z. Huang, *J. Mater. Chem. B* **2013**, *1*, 3202.
- [220] W. Chen, W. Liao, Y. S. Sohn, M. Fadeev, A. Cecconello, R. Nechushtai, I. Willner, *Adv. Funct. Mater.* **2018**, *28*, 1705137.
- [221] W. Chen, G. Luo, Y. S. Sohn, R. Nechushtai, I. Willner, Small 2019, 15, 1900935.
- [222] W. H. Chen, S. Yang Sung, M. Fadeev, A. Cecconello, R. Nechushtai, I. Willner, *Nanoscale* **2018**, *10*, 4650.
- [223] H. Zhao, Q. Zou, S. Sun, C. Yu, X. Zhang, R. Li, Y. Fu, Chem. Sci. 2016, 7, 5294.
- [224] R. Bian, T. Wang, L. Zhang, L. Li, C. Wang, Biomater. Sci. 2015, 3, 1270.
- [225] Y. Li, J. Jin, D. Wang, J. Lv, K. Hou, Y. Liu, C. Chen, Z. Tang, Nano Res. 2018, 11, 3294.
- [226] W. Liu, Y.-M. Wang, Y.-H. Li, S.-J. Cai, X.-B. Yin, X.-W. He, Y.-K. Zhang, *Small* **2017**, *13*, 1603459.
- [227] H. Zhou, C. Fu, X. Chen, L. Tan, J. Yu, Q. Wu, L. Su, Z. Huang, F. Cao, X. Ren, J. Ren, P. Liang, X. Meng, *Biomater. Sci.* **2018**, *6*, 1535.
- [228] F. Shu, D. Lv, X. Song, B. Huang, C. Wang, RSC Adv. 2018, 8, 6581.
- [229] H. Dong, G. Yang, X. Zhang, X. Meng, J. Sheng, X. Sun, Y. Feng, F. Zhang, *Chem. A Eur. J.* **2018**, *24*, 17148.
- [230] L. Zhao, M. Tang, Q. Zhang, Z. Hu, H. Gao, X. Liao, G. Wang, J. Leng, J. Chem. 2018, 2018.
- [231] R. Li, Liu Shichen, Q. Tang, T. Wang, Y. Xie, R. Zhai, Zeitschrift für Anorg. und Allg. Chemie 2018, 644, 317.
- [232] N. Ahmad, H. A. Younus, A. H. Chughtai, K. Van Hecke, M. Danish, Z. Gaoke, F. Verpoort, *Sci. Rep.* **2017**, *7*, 832.
- [233] C. Sun, C. Qin, C. Wang, Z. Su, S. Wang, X. Wang, G. Yang, K. Shao, Y. Lan, E. Wang, *Adv. Mater.* **2011**, *23*, 5629.
- [234] P. P. Bag, D. Wang, Z. Chen, R. Cao, Chem. Commun. 2016, 52, 3669.
- [235] L. Tan, H. Li, Y. Zhou, Y. Zhang, X. Feng, B. Wang, Y. Yang, Small 2015, 11, 3807.
- [236] L. Tan, N. Song, S. X. Zhang, H. Li, B. Wang, Y. Yang, J. Mater. Chem. B 2016, 4, 135.
- [237] J. Fang, Y. Yang, W. Xiao, B. Zheng, Y. Lv, X. Liu, J. Ding, *Nanoscale* **2016**, 8, 3259.
- [238] A. R. Chowdhuri, D. Laha, S. Pal, P. Karmakar, S. K. Sahu, *Dalt. Trans.* **2016**, *45*, 18120.

- [239] X. Gao, M. Zhai, W. Guan, J. Liu, Z. Liu, A. Damirin, ACS Appl. Mater. Interfaces 2017, 9, 3455.
- [240] X. Gao, R. Cui, G. Ji, Z. Liu, Nanoscale 2018, 10, 6205.
- [241] A. Brüning, R. E. Kast, Cell Cycle 2014, 13, 1513.
- [242] X. Lun, J. C. Wells, N. Grinshtein, J. C. King, X. Hao, N. Dang, X. Wang, A. Aman, D. Uehling, A. Datti, J. L. Wrana, J. C. Easaw, A. Luchman, S. Weiss, J. G. Cairncross, D. R. Kaplan, S. M. Robbins, D. L. Senger, *Clin. Cancer Res.* 2016, 22, 3860.
- [243] Z. Skrott, M. Mistrik, K. K. Andersen, S. Friis, D. Majera, J. Gursky, T. Ozdian, J. Bartkova, Z. Turi, P. Moudry, M. Kraus, M. Michalova, J. Vaclavkova, P. Dzubak, I. Vrobel, P. Pouckova, J. Sedlacek, A. Miklovicova, A. Kutt, J. Li, J. Mattova, C. Driessen, Q. P. Dou, J. Olsen, M. Hajduch, B. Cvek6, R. J. Deshaies, J. Bartek, *Nat. Publ. Gr.* 2017, 552, 194.
- [244] M. Wehbe, M. Anantha, M. Shi, A. W. Leung, W. H. Dragowska, L. Sanche, M. B. Bally, *Int J Nanomedicine* **2017**, *12*, 4129.
- [245] M. Wehbe, L. Chernov, K. Chen, M. B. Bally, J. Drug Targeting. 2016, 24, 787.
- [246] X. Zhu, J. Gu, Y. Wang, B. Li, Y. Li, W. Zhao, J. Shi, Chem. Commun. 2014, 50, 8779.
- [247] L. Tian, X. Yi, Z. Dong, J. Xu, C. Liang, Y. Chao, Y. Wang, K. Yang, Z. Liu, *ACS Nano* **2018**, *12*, 11541.
- [248] J. M. Caster, L. Zhang, T. Zhang, L. Huang, A. Z. Wang, Biomaterials 2016, 82, 178.
- [249] B. Lei, M. Wang, Z. Jiang, W. Qi, R. Su, Z. He, ACS Appl. Mater. Interfaces 2018, 10, 16698.
- [250] A. Morris, Nat. Rev. Endocrinol. 2018, 4, 41574.
- [251] T. A. Vahed, M. R. Naimi-Jamal, L. Panahi, New J. Chem. 2018, 42, 11137.
- [252] E. Willenbacher, S. Z. Khan, S. C. A. Mujica, D. Trapani, S. Hussain, D. Wolf, W. Willenbacher, G. Spizzo, A. Seeber, *Int. J. Mol. Sci.* **2019**, *20*, 1808.
- [253] K. Pal, D. Laha, P. K. Parida, S. Roy, S. Bardhan, A. Dutta, K. Jana, P. Karmakar, *J. Nanosci. Nanotechnol.* **2019**, *18*, 1.
- [254] C. He, K. Lu, D. Liu, W. Lin, J. Am. Chem. Soc. 2014, 136, 5181.
- [255] K. Liang, R. Ricco, C. M. Doherty, M. J. Styles, S. Bell, N. Kirby, S. Mudie, D. Haylock, A. J. Hill, C. J. Doonan, P. Falcaro, *Nat. Commun.* **2015**, *6*, 7240.
- [256] M. X. Wu, Y. W. Yang, Adv Mater **2017**, 29, 1606134.
- [257] J. An, S. J. Geib, N. L. Rosi, J. Am. Chem. Soc. **2009**, 131, 8376.
- [258] P. Horcajada, C. Serre, G. Maurin, N. A. Ramsahye, F. Balas, M. Vallet-Regí, M. Sebban, F. Taulelle, G. Férey, *J. Am. Chem. Soc.* **2008**, *130*, 6774.
- [259] W. Cai, H. Gao, C. Chu, X. Wang, J. Wang, P. Zhang, G. Lin, W. Li, G. Liu, X. Chen, ACS Appl. Mater. Interfaces 2017, 9, 2040.
- [260] S. Li, K. Wang, Y. Shi, Y. Cui, B. Chen, B. He, W. Dai, H. Zhang, X. Wang, C. Zhong, H. Wu, Q. Yang, Q. Zhang, *Adv. Funct. Mater.* **2016**, *26*, 2715.
- [261] M. Zheng, S. Liu, X. Guan, Z. Xie, ACS Appl. Mater. Interfaces 2015, 7, 22181.
- [262] J. Zhuang, C. Kuo, L. Chou, D. Liu, E. Weerapana, C. Tsung, ACS Nano 2014, 8, 2812.
- [263] D. Cunha, C. Gaudin, I. Colinet, P. Horcajada, G. Maurin, C. Serre, J. Mater. Chem. B 2013, 1, 1101
- [264] N. Liédana, A. Galve, C. Rubio, C. Téllez, J. Coronas, ACS Appl. Mater. Interfaces 2012, 4, 5016.
- [265] I. Imaz, M. Rubio-Martínez, L. García-Fernández, F. García, D. Ruiz-Molina, J. Hernando, V. Puntes, D. Maspoch, *Chem. Commun.* **2010**, *46*, 4737.
- [266] X. Meng, B. Gui, D. Yuan, M. Zeller, C. Wang, Sci. Adv. 2016, 2, e1600480.
- [267] C. Orellana-Tavra, E. F. Baxter, T. Tian, T. D. Bennett, N. K. H. Slater, A. K. Cheetham, D. Fairen-Jimenez, *Chem. Commun.* **2015**, *51*, 13878.
- [268] M. H. Teplensky, M. Fantham, P. Li, T. C. Wang, J. P. Mehta, L. J. Young, P. Z. Moghadam, J. T. Hupp, O. K. Farha, C. F. Kaminski, D. Fairen-Jimenez, *J. Am. Chem. Soc.* **2017**, *139*, 7522.
- [269] R. R. Der, T. Preiß, P. Hirschle, B. Steinborn, A. Zimpel, M. Ho, J. O. Ra, T. Bein, E. Wagner, S. Wuttke, U. La, *J. Am. Chem. Soc.* **2017**, *139*, 2359.